

A

DISSERTATION REPORT

ON

Design of 1-D photonic crystal filters

is submitted as a partial fulfillment for the degree of

MASTER OF TECHNOLOGY IN WIRELESS AND OPTICAL COMMUNICATION

BY

CHEEPURUPALLI SHIVAJI

(2017PWC5508)

UNDER THE GUIDANCE OF

Dr. Ravi Kumar Maddila



**DEPARTMENT OF ELECTRONICS AND COMMUNICATION
ENGINEERING MALAVIYA NATIONAL INSTITUTE OF TECHNOLOGY
JAIPUR (JUNE 2019)**

CANDIDATE'S DECLARATION

I hereby declare that the work presented in this dissertation entitled, “**Design of 1-D photonic crystal filters**” in partial fulfilment for the award of degree of “**Master of Technology**” with specialization in Wireless and Optical Communication and submitted to the Department of Electronics and Communication Engineering, Malaviya National Institute of Technology is a record of my own investigation carried under the supervision of Dr. Ravi Kumar Maddila, Coordinator and Assistant Professor, Department of Electronics and Communication Engineering, Malaviya National Institute of Technology.

I have not submitted the matter presented in this dissertation anywhere else for the award of any other degree.

Date:
Place: MNIT, Jaipur

CHEEPURUPALLI SHIVAJI
2017PWC5508

CERTIFICATE

This is to certify that the project report entitled “**Design of 1-D photonic crystals**” has been done by Cheepurupalli Shiva,ji, Enrollment No. 2017pwc5508 is an authentic work carried out by him at Malaviya National Institute of Technology,Jaipur under my guidance partial for the fulfillment of degree of Master of Technology in Wireless and Optical Communication during the academic year 2017-2019. The matter embodied in this project work has not been submitted earlier for the award of any degree to the best of my knowledge and belief.

Date:

Dr.R.K.Maddila
Assistant Professor
Department of Electronics and Communication Engineering
Malaviya National Institute of Technology
Jaipur
INDIA 302017

Acknowledgements

I would like to thank all people who have helped and inspired me in the research contributing to this thesis. I take this opportunity to express my sense of gratitude and respect towards my Supervisor of the thesis, Dr. R.K. Maddila, Assistant Professor, Department of Electronics and communication Engineering, Malaviya National Institute of Technology, Jaipur, who has supported and helped to carry out the project. I am thankful to him for all the knowledge he shared with me, without which our research would have been difficult to conclude. In this respect, I find myself lucky to have him as my Project Supervisor.

I also thank all the teaching and non-teaching staffs of the department who have indirectly helped me to complete this project work.

Cheepurupalli Shivaji

Abstract

The bandgap in the 1-D plasma photonic crystals (PPCs) which is known as photonic bandgap have been studied numerically using the finite-element method. The photonic bandgap of 1-D PPCs is due to the effect of plasma density. A photonic crystal is designed with plasma inscribed in it and electromagnetic waves are made to pass through the crystal in one direction. The characteristics of the 1-D PPCs is observed by varying the plasma density along. The permittivity of the plasma is varied with plasma density depending on the variation of the frequency of the electromagnetic waves. The microwaves propagating through the 1-D PPCs are examined for their transmission characteristics. The adverse TE mode PBG structure of 1-D PPCs has been produced under the cutoff area, i.e. in the low frequency region. In conditions beyond the cut-off region, i.e. in the high-frequency region with the air acting as the high-dielectric constant slab and the plasma placed into the quartz pipes, the formation of PBG is associated with the periodic dispersion of the EM wave at the plasma surface. The changes in the plasma density leads to the change in the PBG structure. If the modifications produced in plasma density are significant, PBG created at the circumstances close to the cutoff frequency area can be eliminated. A photonic crystal filter with plasma at regular intervals is formed and its characteristics are observed. An effort is made to design a photonic crystal filter with air inserted in it is designed and observe its characteristics.

Contents

Abstract	iv
Contents	v
List of Figures	vii
List of Tables	ix
Nomenclature	ix
1 Introduction	1
1.1 Plasma	2
1.2 Photonic crystals	3
1.3 Types of PhCs	3
1.4 Photonic bandgap (PBG)	5
1.5 Photonic crystals in the nature	6
2 Literature Survey	8
3 Plasma Photonic crystal	16
3.1 Introduction	16
3.2 Plasma Photonic Crystal	16
3.3 EM wave propagation in PhCs	17
3.4 Boundary conditions	18
3.5 Methods of computing	20
3.6 Computational model of 1D plasma photonic crystal	25
3.7 Photonic Crystal filters	26

4	Simulation & Results	27
4.1	Designing parameters	27
4.2	Structure of the photonic crystal and simulations	28
4.3	Quasi modes	32
4.4	Variations in the permittivity of the plasma photonic crystal	42
4.5	Bandgap variations for various plasma densities	43
5	Conclusion and Future work	45
	Bibliography	47

List of Figures

1.1	1D photonic crystals can consist of deposited or fastened layers.	4
1.2	It is possible to make two-dimensional objects by photolithography or by drilling holes in a appropriate substratum.	4
1.3	3D manufacturing techniques include drilling under various angles, stacking various 2-D layers on top of each other, direct laser writing, or, for instance, instigating self-assembly of spheres in a matrix and dissolving spheres	4
1.4	The opal in the above bracelet has a natural micro photonic structure that is accountable for the iridescent color	7
1.5	Diamonds in the rough: the Brazilin beetle <i>Lamprocyphus augustus</i> (top) has scales containing photonic crystal that give the insect its unique green shimmer. Because of microscopic diamonds, individual scales on the beetle reflect iridescent green – like structures.	7
3.1	Schematic of 1-D PPCs which is to be designed.	25
4.1	Strucure of the photonic crystal designed in comsol with five quartz tubes filled with plasma.	28
4.2	1-D PPC at first eigen frequency.	29
4.3	1-D PPC at second eigen frequency.	30
4.4	1-D PPC at third eigen frequency.	30
4.5	1-D PPC at fourth eigen frequency	31
4.6	1-D PPC at fifth eigen frequency.	31
4.7	convergence plot.	32
4.8	1-D PPC at sixth eigen frequency.	33
4.9	1-D PPC at seventh eigen frequency.	34
4.10	1-D PPC at eighth eigen frequency.	34

LIST OF FIGURES

4.11 1-D PPC at ninth eigen frequency.	35
4.12 1-D PPC at tenth eigen frequency.	35
4.13 1-D PPC at first eigen frequency with polariztion.	36
4.14 1-D PPC at second eigen frequency with polariztion.	37
4.15 1-D PPC at third eigen frequency with polariztion.	37
4.16 1-D PPC at fourth eigen frequency with polariztion.	38
4.17 1-D PPC at fifth eigen frequency with polariztion.	38
4.18 1-D PPC at sixth eigen frequency with polariztion.	39
4.19 1-D PPC at seventh eigen frequency with polariztion.	40
4.20 1-D PPC at eighth eigen frequency with polariztion.	40
4.21 1-D PPC at ninth eigen frequency with polariztion.	41
4.22 1-D PPC at tenth eigen frequency with polariztion.	41
4.23 For various plasma densities the real components of the relative permit- tivity.	42
4.24 For various plasma densities the simulated bandgap is given.	43
4.25 The photonic crystal structure when plasma is replaced with air	44
4.26 The photonic crystal structure when plasma is replaced with air.	44

List of Tables

3.1	Definition of symbols in wave equation	21
3.2	values of s_y and s_z	21
4.1	Parameters used in the design of waveguide	27

Chapter 1

Introduction

Metallic diffraction gratings and cavities are extensively used to control the spread of microwaves. Metallic chamber walls restrict the transmission of radio waves under a certain frequency threshold at frequencies, and the metallic waveguide enables transmission across its axis only. Scientists later thought that regulating the propagation of electromagnetic radiation beyond the microwave zone, such as visible light region, would be very helpful. It is hard to generalize the metallic diffraction grating and cavity approach to the optical wavelengths by dispersing infrared light energy within metallic sections. Researchers then switched to photonic crystals (PhCs) that enable the generalization and scaling of cavity and wave guide characteristics to cover wider frequency ranges. For microwave influence with millimeter dimensions or micron sizes for in-fared control, a photonic crystal of specified composition can be produced. The parameters that determine the width and role of PBGs, like permittivity and constant lattice, have always been difficult to change in a photonic crystal. There's so much focus to the photonic crystals that are composed of different types of conductive material that operate at the visible spectrum.

Many researchers have been keen to introduce plasma in to the PCs to control EM signal transmission propagation features in PCs in latest years. The plasma-based PhCs, known as PPC, have distinctive characteristics because of plasma presence. The PPC's photonic bandgap is influenced by the Plasma density. In PPCs, plasma dielectric strength varies between negative and favourable values of less than unity, based on the wavelength of the EM wave signal and plasma densities.

1.1 Plasma

A warm electrically charged gas composed of about equal amounts of electrons that are negatively charged and positive ions is described as plasma. Plasma is considered as a distinct fourth state matter after solid, liquid and gas due to its unique characteristics which are different from that of ordinary neutral gases. Plasmas are heavily affected by electromagnetic and evanescent waves as they consist of ionized particles. In contrast to the internal or external used areas of science, the plasma is operated by electric and magnetical fields, generated by electric and widely distributed charge levels that result from the differential motion of electrons and ions within the plasma as a whole. The energies imposed by these areas on the charging particles that form plasma are produced to behave over lengthy spans and to give a consistent, collective value to the conduct of the electrons not showing neutral gases.

The presence of electrical potential and highly concentrated charging levels do not influence the plasma's neutral nature because plasma remains always electrically "quasi-neutral," as there are roughly equal numbers of positive charged particles and electrically charged particles distributed to cancel charges. There is an estimation that around 99% of the matter in the universe is in the plasma state...hence the expression plasma universe. The examples of astrophysical plasma are stellar, stars extragalactical jets and the interstellar medium. The Sun consists of plasmas in our universe, magnetospheres, the interstellar medium and ionospheric planets, as well as the asteroid ionospheres and other planetary system.

The plasmas which interest space physicists, the density is significantly less than in experimental vacuums. The plasmas are extremely tight. The temperature ranges from several thousand degrees Celsius in the plasmasphere to many million degrees in space plasmas are extremely high. The tempratue of the ionosphere-based "cooler" plasmas is typically reflected in the temperatures of the Kelvin degrees, and of the "warmer" magnetosphere-bodied plasma are more frequently reflected in the average age kinetic energy of their constituent elements measured in the electron volts. Magnetospheric plasmas are often described as "cold" or "hot." By adding energy to a gas, plasma is developed so that some of its electrons leave its atoms. This is known as ionization. It results in electrons charged negatively and ions charged positively.

1.2 Photonic crystals

A photonic crystal is a regular optical nanostructure that impacts photon movement in much the same manner that ionic lattices influence solid electrons. Photonic crystals (PhCs) have been widely researched for their outstanding capacity to regulate electromagnetic (EM) waves. PhCs give a versatile way to regulate light emission and propagation, and the light-matter interaction resistance can be customized by varying, for instance, the structure's lattice constant.

PhCs are artificial substances that influence photons in a way similar to that shown by semi-conductors on electrons. They have a photonic bandgap that does not spread photons of certain energy in the crystal, regardless of which way of polarization and propagation. The PhCs are characterized by three parameters: arrangement of the grids, space period and the dielectric constants of the component material. By choosing these parameters carefully, we can create a gap in which the propagation of a specific range of electromagnetic waves is prohibited. This prohibited frequency range is referred to as photonic band gap.

1.3 Types of PhCs

PhCs are basically classified into three major types depending upon the periodicity that is introduced into the structure and they exhibit different types of characteristics. They are :

- (a) 1D Photonic crystals.
- (b) 2D Photonic crystals.
- (c) 3D Photonic crystals.

PC's lattices illustrations composed of a regular dielectric constant variation, depicted as a color shift. Each and every photonic crystal, even the simplest has surprising properties which is constructed to reflect light that is being incident from any polarisation. This kind of reflectors are known as Omnidirectional reflectors. Let us assume that a photonic crystal prevents the propagation of certain frequencies from the electro-magnets of any polarizing wave traveling in a given direction, and then we say that now the crystal has the complete photonic band gap.

We can not have a complete band gap in a 1D PhC, since the material interactions occur in one axis. Omnidirectional reflectors can be built but only for light sources

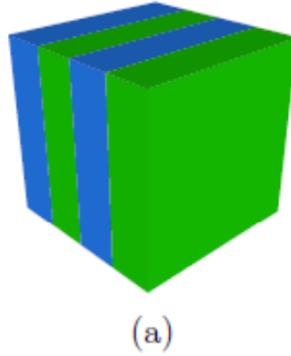


Figure 1.1: 1D photonic crystals can consist of deposited or fastened layers.

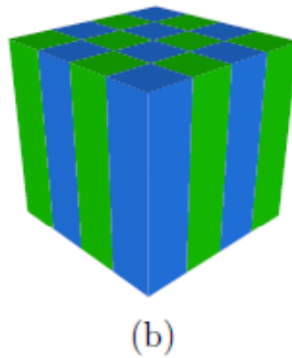


Figure 1.2: It is possible to make two-dimensional objects by photolithography or by drilling holes in a appropriate substratum.

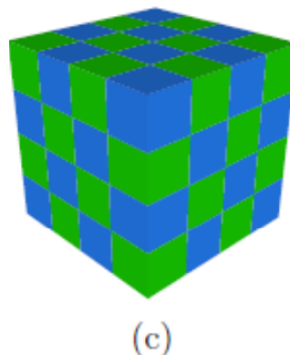


Figure 1.3: 3D manufacturing techniques include drilling under various angles, stacking various 2-D layers on top of each other, direct laser writing, or, for instance, instigating self-assembly of spheres in a matrix and dissolving spheres

which are at greater distances from the PhCs. A 3D PhC with a wide variety of dielectric constants is better suited to create a complete photonic band gap whose dielectric grid must be periodically on the three axes.

For the first time in 1887 studies were conducted on electromagnetic field propagation through periodic materials by Lord Reyleigh. Rayleigh noted thin bandgaps prohibiting the spread of light. The crystal was discovered to correspond to a periodic one-dimensional (1D) lattice preventing the electromagnetic radiation by passing the material due to the toa-resonance impact. With the result of this breakthrough, dielectric stacks were used to create multifaced thin films. The door was opened.

The notion of Yablonovitch and John was to use photon crystals to obtain more efficient optic devices which work at optic wavelengths, including semiconductor lasers, and baptisms in height. In 1987 the optical analog to semiconductor material were suggested by Yablonovitch and John, introducing the concept of mixing classical electromagnets and solid-state physics into omnidirectional PBG. Spontaneous emission in unwanted directions leads to significant loss in all these appliances. PBGs produced by PCs were proposed to eliminate undesirable spontaneous emissions while improving the selected directional emissions. Based on the quantum influence of electron location on semiconductors, it was stressed that specific failures incorporated in an existing PhC could support localisation modes which would allow PBG's surrounding light to trap. Since these landmarks research has started explosioning in theoretical simulation and the physical implementation of these artificial materials. The traditional limits of conventional manufacturing processes, together with the creation of new state-of - the art nanometer techniques were developed to achieve 1D, 2D and 3D photonic crystal resolution nanometers.

1.4 Photonic bandgap (PBG)

As we have worked only on one dimensional photonic crystal, here we will limit our discussion to one dimensional photonic crystal only. A 1D PhC is composed of layers that are dielectrically-alternated the same as the wavelength of light in this system repeats period a , in the z -direction. This scheme repeats with period a , in the z -direction, and the periodicity will be in the order of the wavelength of the light. An aerial wave that travels in Z -direction across the periodicity line will be dispersed at the intersection between two parts. This causes the waves in the framework to spread forward and backwards. Such waves will now intervene and cause standing waves to form.

In an isotropic material dispersion equation of light is given by

$$\omega(k) = \frac{ck}{\sqrt{\epsilon}} \quad (1.1)$$

where c is the speed of light,

k is a wave vector and

ϵ is a dielectric constant

This equation shows that light energy varies linearly with momentum, zero energy provides us zero momentum. In the figures the dispersion relation of a photonic crystal of one dimension is plotted. The figure 1.1 has two dielectric layers with same dielectric constant. The figure 1.2 has the difference between the two dielectric constants as one. The figure 1.3 had the difference between the two dielectric constants as twelve. In many aspects (a) (b) (c) of the figure... are same but there is a region of frequency that do not contain photonic modes, which is called as photonic band gap. This bandgap is due to the difference in energy field location.

where k is $k = \frac{\pi}{a}$

1.5 Photonic crystals in the nature

Gemstone opal is a well known natural photonic crystal. The opal's variable colors lead from a photonic crystal phenomenon depending on the crystal lattice planes' diffraction of light by Bragg. An unusual way of showing luminescent green from all points of view was discovered for a Brazilian beetle species. The beetle-size structure was found to be an ideal photonic crystal (carbon-based structure) with a recurring unit arrangement of roughly 300 nm for visible light. Diamond-based structure is thought to be the most efficient 3D periodic structure for visible spectrum because a large variety of colors can very much be reflected. The visible structure of Such a light is a challenge for scientists to produce from appropriate materials, given the need for a very tiny structural periodicity.



Figure 1.4: The opal in the above bracelet has a natural micro photonic structure that is accountable for the iridescent color



Figure 1.5: Diamonds in the rough: the Brazilin beetle *Lamprocyphus augustus* (top) has scales containing photonic crystal that give the insect its unique green shimmer. Because of microscopic diamonds, individual scales on the beetle reflect iridescent green – like structures.

Chapter 2

Literature Survey

S. John, et al. “Strong localization of photons” [1987] [1]. It has been shown that in some disordered superlattice micro-structures with sufficiently high enough dielectric constant, strong photon localization can occur in a very highly predictable manner for a particular frequency window. The materials mentioned are comparable to amorphous semiconductors in which there will be an interference between order and disorder that results in a limitation of coherent back-scattering for a certain Bragg resonance channel. These considerations are produced in the hope that they will provide guidance for the experimental quest to locate the photon. This use of photon localization as a trigger mechanism for nonlinear or bi-stable response leads to a number of useful device applications.

E. Yablonovitch, et al. “Inhibited spontaneous emission” [1987] [2]. It was found that uninhibited atomic emissions arising from the interaction of matter with space are not always a fixed and unchangeable characteristic. By altering the radiation field, this uninhibited emissions can be regulated. The efficiency is restricted by this inhibited emission in semitransparent laser, solar panel and bipolar transistors. The unrestrained emission can be carefully prohibited in a periodical 3D dielectric structure with an electromagnetic band gap intersecting with the electronic band. The periodic spatial modulation opens a forbidden gap in the electromagnetic diffusion connection, at least for the horizontal spread of light into the layers.

S. P. Kuo, et al. “Interaction of an electromagnetic wave” [1997] [3]. The interaction of electromagnetic waves with quickly generated spatially regular time-varying plasmas is being researched. The numerical findings of the collision-free situation indicate

that upshifted frequency as well as downshifted frequency waves both are produced. Here plasma is blocking the frequency downshifted waves with lesser frequencies than that of the plasma frequency. The impact of trapping is to dramatically increase the effectiveness of the downshift frequency conversion method by accumulating incident wave energy during the plasma transition period. A theory is developed based on the wave impedance of the regular structure of each Floquet mode, incorporating the plasma's collisional damping. A theory relied on the wave impedance of each regular Floquet mode where the downshifted frequency signals were identified repetitively with significantly increased spectral intensities while the upshifted frequency signals were completely removed. An extra phenomenon found in the tests is the unexpected downshift of the frequency along with the upshift of the frequency resulting in the fresh pulse being spectrally broken. The dispersion relationship is obtained from the propagation of an electromagnetic wave in a regular plasma medium. The dispersion relationship is obtained from the propagation of an electromagnetic wave in a regular plasma medium. Between two adjacent branches of the frequency curves there exists a frequency gap which is known as band gap. The impedance description offers a physical insight into why only the downshifted frequency signals were detected repeatedly in the experiments. These downshifted frequencies are found with significantly increased spectral intensities while the measurements couldn't find the frequency upshifted signals.

M. Koshiha, et al. "Full-vector analysis of photonic crystal" [2002] [4]. A full vector numerical analysis method which is required for the accurate modeling of photonic crystal fiber is presented. The behavior of index guiding PCF, also called Holey Fiber (HF), is precisely analysed based on BEM known as the Boundary Element Method, which is a complete vector boundary element technique. The containment loss is assessed with the calculation of the complicated efficient HF coefficient along with the measurement of the complete HF distribution. Birefringence for HF with BEM is also evaluated. HF is generally a single-material optical fiber, with periodic air trough arrangements running throughout its entire length. The distribution of design parameters in the coating region provides great flexibility which opens up a great potential for the design of fibers with unique properties, which do not have heat transfer fibres. The BEM nature makes it very simple to create a mesh as opposed to techniques such as FEM involving the entire domain because of the inclusion on borders. Consequently this method provides results in a very small amount of time as the size of final matrix is smaller in comparison with that of FEM. Green's function takes into account the field at unlimited distance,

which results in another distinct advantage in the comparison of this technique with other numeric methods such as FDTD and FEM, where the boundary conditions that are embedded are to be observed. The testing of the amount as well as trough size and the wavelength of air-holes causes the loss of containment. By varying geometrical parameters for different wavelengths the group velocity is calculated. By varying the size of holes inscribed in the structure Birefringence behavior of HF is investigated.

H. M. H. Chong, et al. "Tuning of photonic crystal waveguide" [2004] [5]. At $\lambda = 1530$ nm a photonic crystal microcavity which is tunable consisting of in filling holes is realized through experiment with the help of thermo-optic effect in a silicon insulator waveguide. In order to obtain a very high confinement vertically the device has been fabricated with reactive ion etching in the silicon core layer. The photonic crystal microcavity has been integrated with a thin film heater. A minute change in temperature leads to a change of refractive index which is good enough to make a notable change in resonance. The heater has a switching power around 9mW which is switched to generate a 1.2mA current which gradually achieved a shift in the resonance of 5nm. Finally, they proved how a thermo-optical impact is achieved by a photonic crystal microcavity H2. In the experiment, the Q-performing microcavity was maintained very high, and the maximum resonant wavelength 5 nm with a 9.2 mW power consumption was controlled. They were also aware of the fact that the necessary switching force could be lowered by a factor of three because the heater electrode covered the cavity along the propagation axis about three times. They also indicated that this device has the potential for the applications like wavelength division multiplexing and demultiplexing and can act as a photonic switch due to the low power requirement for substantial tuning.

H. Hojo, et al. "Dispersion relation of electromagnetic waves" [2004] [6]. Studies have been performed to achieve an electromagnetic wave distribution relationship with a 1D photonic crystal plasma. The plasma photonic crystal described is a periodic arrangement of the thin plasma and dielectric material in a rotated manner. The Maxwell equation is resolved using a technique similar to the problems of the Kronig-Penny quantum mechanics, so that the dispersion relationship is obtained. The one-dimensional photonic crystal the dispersion relation is computed in the same way as the power band is measured in photonic crystals and the band structures anticipated to emerge in the dispersion relationship between electro-magnetic waves in onedimensional photonic plasma crystals. They noticed that the phase speed decreases for a bigger dielectrical constant value and also that the phase speed decreases as the frequency difference for a smaller

plasma width increases, when the width of the dielectric materials is fixed. Studies have been performed to achieve an electromagnetic wave distribution relationship with a 1D photonic crystal plasma. They can lastly be used for new plasma functional instruments like frequency filters for millimeter wavelength ranges.

M. Qiu, et al. “Photonic band structures for surface waves” [2005] [7]. Surface plasmon waves (SPW) are the spreading power waves which are bound to the metal dielectric interface and which are produced by surface plasmons. Surface plasmon waves are the waves of the electromagnetic ground which spread along a dielectric structure. Normally an operating system between (PEC) and the dielectric may not support the surface waves since electro-magnetic fields can not enter the ideal conductor. The holes in the framework enable electromagnetic fields to enter the structure by creating PEC surfaces that support the superficial waves in one dimension (1D) and two dimensional (2D). These surface waves and the standard surface waves effectively are responsible for certain extraordinary metal optics (i.e., a high transmission through the subwavelength holes in metal film). These waves have an extraordinary metal connector optics. Vectorial finite difference time method used to achieve photonic surface band structures on structured metals with a periodic hollow structure on structured metal surfaces. One can always obtain a surface mode for different types of lattice structures formed by varying the size, shape and depth of holes. They were also in excellent agreement with the exterior outcomes received for a square box of wood in the shape of wax in brass. They also demonstrated that holes in the structure may serve as cavities for the structured surfaces composed of a finite depth. They have noted the presence of propagating coupled cavity modes which are having a low group velocity, confined to the surface and is decaying exponentially into the dielectric above. They showed that for all cases there are surface methods: cylindrical square box holes, cylindrical square holes and cylindrical triangular holes that are strictly limited to the surface that are both in the background and in their holes exponentially deteriorating

O. Sakai, et al. “Interaction and control of millimetre-waves” [2005] [8]. In this paper three experimental results were discussed. The transmission of electromagnetic waves in a range of 10-75 GHz was experimentally investigated in several types of microplasmas. A Drude type model is used to derive the electron density by comparing the transmittance with collisional effects and by using the planar geometry of the microplasma assembly the fundamental characteristics of the propagation were investigated. An outstanding propagation pattern such as the localizing impact was observed

in a two-dimensional regular microplasma array. The type of anomalous refraction can not be interpreted by only predictions based on the dielectrical properties of bulk plasma and a periodical dielectric structure similar to photonic-crystal may play an significant role. It has been shown that the T-junction created by a microplasma which is connected to a microstrip line is capable of controlling microwave transmission. Two T junctions in sequence have to be linked to the right corner of a strip line to achieve a depth of attenuation (or modulation) of approx 35 percent. All these characteristics are achieved with a comparatively elevated electron density of 10^{13}cm^{-3} . All these features are obtained by maintaining relatively high electron density of the microplasmas near 10^{13}cm^{-3} . The total size of microplasmas varies from several millimeter to a submillimeter depending on the microwave wavelength range from a few tens of gigahertz to tetrahertz. The spread of waves through the 2D square array plasma pillars extending from the mesh scheme has been analyzed. New structural characteristics found, not only are the attenuation but also omnidirectional refraction and distortion of rays. Experimentally, this impact shows for the first moment that a microplasma array grid structure is similar to that of powerful dielectrics as a photonic glass. Finally, it has shown that the propagating microwave transmission can be regulated by complex T connections produced by micro plasmas between coplanar discharges and microstrip lines.

L. Shiveshwari, et al. "Photonic band gap effect" [2006] [9]. The forbidden frequency regions which appear in a periodically structured photonic crystal are known as Photonic Bandgaps. The development of 1D 2D and 3D photonic crystals lead to the thought of using photonic devices which had and will further revolution the field of photonics analogous to the contribution of semiconductors in the field of electronics. 1D plasma dielectric photonic crystal is a regular array of continuous plasma and dielectric material by which a wave is propagating electromagnetic and by means of a process comparable as Kronig-Penny's (KP) model of quantum mechanics the band structure is discussed. Transmission and reflection coefficients which are required for the complete transmission in 1D plasma dielectric photonic crystal are calculated. They obtained photonic band gap characteristics even for smaller variations in the periodicity. Air plasma photonic crystals have been studied to come to know that more number of unit cells are required to get a better transmission minima. The band features are created and according to the differences in plasma layer thickness and density the band gap is changing obviously suggests that the PBG impacts are caused by the overall connection between distinct plasma layer unit cells. Once the plasma thickness is in the

micrometer and mm range, the plasma PCs give major benefits for filters and other plasma functional equipment.

S. Prasad, et al. “Effect of inhomogeneous plasma density” [2011] [10]. The reflectivity of a plasma photonic crystal depends on the non homogeneous nature of plasma density. Thus, the one is exponentially different in two plasma-density profiles, while the other is linearly diversified so that the average volume permittivity remains constant. A transfer matrix method is used for the distribution relation and reflectivity of the specified buildings using the continuity circumstances of the electric fields and their derivatives on the interface. The exponentially different plasma density gives very high reflection in comparison with the linearly different plasma permeability profile for all of the studied cases. When the two profiles are compared. The plasma thickness distribution is exponentially different and perfectly reflects a considered average volume permittiveness. In sensor apps and plasma functional devices, this profile can also be used. With regard to plasma, it is important to really examine the interaction of electromagnetic waves with plasma for years in several areas such as plasma fusion, ionospheric and plasma reactors.

J. Kitagawa, et al. “THz wave propagation” [2012] [11]. The transmission and dispersion relationship for THz Waves in a two-dimensional photonic crystal consisting of metallic rods are studied by means of Finite-difference time-domains and measurement for THz time-domain spectroscopy. The objective of THz PCs is the creation of a low-loss waveguide and a high-quality resonator with high function PCs such as an optical module modulator or a mechanical tunable filter which are still under development. The photonic band gap will be removed if the air gap is two to three times the rod height. On the other side, with the air gap reduced to less than $50 \mu\text{m}$ the PBG methodically increases. In addition to the technical lateral stiffness of PBG, the modifications from 2D to 1D have enhanced PPWG with unheated differences.

B. Guo, et al. “Photonic band structures” [2012] [12]. The PBSs for angled transmission in 1D plasma photonic crystal are calculated. photonic band structures are calculated. The photonic crystal acts as an anisotropic (varies according to its directions) if the plasma glazing constant, which is doped into the pc is smaller compared to the wavelength of the incidence. As a result, the dielectric constant becomes a dielectric tensor constant that determines PC PBSs. Changed the voltage, gas pressure and temperature is governed by plasma. Plasmas can serve as dielectric, metal or even

a fresh material with unexplained physical parameters, since they are dispersive media for loss. The effects on plasma-bond structure and optical features of a Plasma PC were investigated by multiple parameters, such as plasma frequency (plasma density), plasma layer thickness, and internal magnetized fields. With the assistance of the transmission matrix method they have implemented an analytical technique to study the angle incidence propagation of the occurrence in the 1D PhCs. The relationship of the plasma loading factor is calculated according to the efficient dielectric constant of PCs as well as normal and up take PBSs. In conclusion, the incorporation of plasma into photonic crystals will significantly strengthen theoretical and laboratory opportunities for studies in PCs.

L. Qi, et al. “One-dimensional plasma photonic crystals with sinusoidal densities,” [2014] [13]. The characteristics of electromagnetic interferences are explored with ordinary and oblique incidences for 1D plasma layers with sinusoidal densities. The photonic bandgap features for photonic crystals are used as a product of wave frequency transmission. Increased frequency of collision is shown to increase concentration for regular structures, to boost the modulation aspect, to rise gap size and to increase the angle of incidence, the position of the gaps for both polarizations can change. A defective layer could be implemented by inserting a fresh plasma layer in the center, which can cause a defect mode to appear in the gap. The angle of propagation allows the frequency to be tuned. The density of the defect layer affects the number and frequency of defect modes and results help to design narrow band filters for tuning.

J. Luo et al., “Ultratransparent media and transformation optics” [2016] [14]. Thanks to the overall property of reflection induced by the impedance mismatch transparency in natural products such as dielectrical products has never become ideal. In these last few years photonic crystals have been suggested to perform unusual electromagnetic characteristics beyond natural materials, which are deemed unnatural electromagnetic structures and superconducting materials. For Pure Dielectric PhCs the spatial dispersion parameters were used to create the perfect transparent media with an omnidirectional impedance that allows 100 percent light transfer in all angles. These phcs have been assigned for elliptical contours of equal frequency (EFCs) and are moved in k range with powerful spatial dispersion. These photonic crystals enable maximum light to pass through certain frequency regimes, forming certain virtual pictures free of aberration which make these ultra-transparent media more than ordinary, transparent media like dielectrics. With the diffusing waves in the dissipation media, the dispersion

and surface impedance of own countries in the photonic crystal can be acquired, which are efficient and dependent on K . We first notice the band that shows changed EFCs in the band structure. By altering the microstructure of photonic crystals, this band change can be regulated. The designing process is much easier for the incident angles whose range is very small.

Haiyun Tan, et al. "Simulation on the Photonic Bandgap of 1-D Plasma Photonic Crystals," [2018] [18]. They examined the transmission characteristics of the 1-D PPC microwaves and confirm that the bandgaps of all PPCs are heavily dependent on the plasma density. The adverse PBG model TE mode of the 1D PPCs is generated similar to the metal PCs in areas with a low frequency below the cutoff frequency. The PBG of surface modes and another series of constant Fanomodes generate a pass band broad in the cut-off area, a number of sharp transmittance peaks. On the other hand, the high frequency area under conditions beyond the cutoff frequency, with air behaving as a high-dielectric constant slab, the properties of 1-D PPCs will be similar to those of the conventional PCs, with plasma holes continuing to act as the material of lower dielectric constant where PBG formation is linked to periodic dispersion of EM waves in the plasma surface. In contrast, the PBG formed under the conditions near the cut-off frequency, which related to the change in the plasma dielectric constant, where all PBGs therein are controlled by plasma, can be mutated. Finally, with the characterisation of these PPCs we will be able to build the same types of devices and to comprehend how EM waves and plasma interact to enrich PC science.

Chapter 3

Plasma Photonic crystal

3.1 Introduction

In latest years, photonic crystals have been intensively examined because of the uniqueness of the electromagnetic characteristics and the possible applications. The photonic bandgaps were created as a consequence of Bragg's intrusion in a continuous dielectric framework. In a photonic crystal, it is difficult to change the variables determining the PBG's width and position, like the permitability and grid constancies. The photonic crystals of different sorts of dielectrics work in the visible wavelength. There is just too much attention. The study into photonic crystals was expanded to plasma photonic crystals with the improvements of plasma engineering technology. In order to transmit data through large distances while maintaining high data rates we need all optical communication networks. This network involves optical devices like optical demultiplexers, optical switches and optical filters etc. The ability of the photonic crystals to control light even in ultrasmall (uncomparable) dimensions makes them suitable for design of optical filters.

3.2 Plasma Photonic Crystal

PPCs with better features than standard photonic crystals, operated on the microwave band (MW). Plasma is a ionization medium of the frequency of electromagnetic waves that will transmit through the medium, which gives PPCs many new features as regards normal photonic crystals. The frequency range of electromagnetic waves for ordinary, strong material photonic crystals to manage is fixed when photonic crystals are manufactured as parameters that determine the width and position of PBGs, for example

permittivity and threshold constant, are hard to alter. In PPCs, these parameters can be freely diverse to make it independent to varying demands by changing internal parameters together with those parameters.. Kuo and Faith [3] first derived the equation for dispersion in 1D PPCs by applying Bloch's theorem. Shiveshwari and Mahto [9] made the theoretical analysis for the transmission coefficients and the reflection coefficients and bandgaps in 1D PPC in terms of plasma density, plasma width, and number of unit cells. Guo et al. [12] analyzed the photonic band structures for 1D PPCs with the time-variation in plasma density and found that band structures can be tuned by changing the time which is going to modify the plasma permittivity in different frequency regions. Sakai et al.[8] analyzed band structure of 2D PPCs which interact with different polarized waves and observed its bandgap in the Γ -X direction around a frequency of 60 GHz experimentally.

Studies in the past have demonstrated, in a vacuum system, that plasma units in PPCs are usually produced to keep a correct release that limits the PPCs from being used as a handy microwave device (i.e. plasma plates in 1D or 2D plasma columns). The dielectric barrier discharges (DBD), which can produce the independently-organized plasma structures or the use of Micro-Hollow Cathode discharges (MHCDs), is often used to form 1D and 2D PPCs, are used to regulate transmission on electromagnetic waves. But it is traditionally difficult to manage the homogenous material or the uncertainty of the discharge. Different PPC discharge conditions and dimensions were explored for the characteristics of the PPCs. The FDTD technique has been used to analyze the transmission over the 1D PPCs of microwaves.

3.3 EM wave propagation in PhCs

Maxwell's equations describe the spread of the EM wave through a photonic crystal. A linear mixture of transversal electrical field (TE) and transversal magnetic field (TM) is always an electrical field or magnetic field. Here there are two cases, in the first case, the electric field is sensitive to the photonic crystal plane and the magnetic field is entirely limited to this plane. For an electric field the Helmholtz equation into which the source less Maxwell's equations are reduced is given by

$$\nabla^2 E_z(\vec{r}) + k_0^2 \epsilon_r(\vec{r}) E_z(\vec{r}) = 0 \quad (3.1)$$

$E_z(\vec{r})$: z-th component of the electric field at position (\vec{r}),

$\epsilon_r(\vec{r})$: in-homogeneous relative dielectric constant of the PhC,

and $K_0 = \frac{\omega}{c}$ where ω : the angular frequency of the incident E field and c : the velocity of the light in free space.

In the above equation the photonic crystal is assumed to be non-magnetic ($\mu_r = 0$) and non-conducting as well ($\sigma = 0$), after solving the above equation the time-harmonic magnetic and electric fields are obtained as below

$$\vec{E}(\vec{r}, t) = E_z(\vec{r})exp(-i\omega t)\hat{z} \quad (3.2)$$

$$\vec{H}(\vec{r}, t) = \frac{i}{k_0} \nabla \times \epsilon_r(\vec{r})\vec{E}(\vec{r}, t) \quad (3.3)$$

In the other condition for TM polarization, the magnetic field will be perpendicular to the plane of the photonic crystal and the electric field is restricted into the plane therefore the source less maxwell's equations have been reduced to the Helmholtz for a given magnetic field by

$$\nabla \left(\frac{\nabla H_z(\vec{r})}{\epsilon_r(\vec{r})} \right) - k_0^2 H_z(\vec{r}) = 0 \quad (3.4)$$

$H_z(\vec{r})$ is the z-th component of the electric field at position (\vec{r}).

After solving the above equation the time-harmonic magnetic and electric fields are easily calculated as below

$$\vec{H}(\vec{r}, t) = H_z(\vec{r})exp(-i\omega t)\hat{z} \quad (3.5)$$

$$\vec{E}(\vec{r}, t) = -\frac{i}{k_0\epsilon_r(\vec{r})} \nabla \times \vec{H}(\vec{r}, t) \quad (3.6)$$

3.4 Boundary conditions

The most significant element in an electromagnetic simulation is the use of adequate interface boundary conditions. For the calculations of the photonic band structure as shown below, the limits and conditions which are to function as an unbounded domain for simulation combined with the photonic crystal lattice period are to be implemented. We need a perfect magnetic conductor (PMC) or a perfect electric condition (PEC) to fulfill the simulation field in order to simulate an infinite medium. For transverse electric (TE) polarisation of the EM field, the perfect magnetic state is used which ensures that the tangent magnetical field component of the external interface is identically null and

is given by

$$\hat{n} \times \vec{H} = \vec{0} \quad (3.7)$$

\hat{n} : A perpendicular unit vector to a surface of the external simulation field at every stage.

The ideal electrical situation (PEC) is used to polarize the EM field transverse magnetic (TM) and ensures that the element of the power field tangential to the border is equally zero at the outer border.

$$\hat{n} \times \vec{E} = \vec{0} \quad (3.8)$$

The periodicity is assured by proper use of the Bloch theorem at the boundaries of the photonic crystal unit cell for the photonic crystal grid. This theorem says that the only impact for the EM field is to alter in its stage for TE and TM respectively if the electrical field or magnet field propagates on the PC from one spot to another spot in a PC that is segregated from the prior one by a lattice vector, \vec{R} .

$$E_z(\vec{r} + \vec{R}) = \exp(i\vec{k} \cdot \vec{R})E_z(\vec{r}) \quad (3.9)$$

and

$$H_z(\vec{r} + \vec{R}) = \exp(i\vec{k} \cdot \vec{R})H_z(\vec{r}) \quad (3.10)$$

\vec{R} : A vector of the PhC lattice,

and \vec{k} : The wave-vector of the electromagnetic wave.

Along with this for calculating the transmittance which is represented below, the finite clusters are used which are in the direction of the incident wave vector are used and the clusters are infinitely extended in the direction perpendicular. PMC and PEC boundary environments at the external implementations are used in order to reproduce such material, limiting the computation domain to the incident wave vector vertical to TE and TM polarisation. In order to avoid spherically symmetric reflection due to the relatively limited size of the constellation and therefore perfectly adapted layers have been utilized on such interfaces, the condition is a little more engaged for those interfaces at which the EM wave enters and exits the cluster. The equations that describe such limits are provided as follows

$$\hat{z} \cdot \hat{n} \times (\nabla \times E_z \hat{z}) - i\beta E_z = -2i\beta E_{0z} \quad (3.11)$$

and

$$\hat{z} \cdot \hat{n} \times (\nabla \times E_z \hat{z}) - i\beta E_z = -2i\beta H_{0z} \quad (3.12)$$

where E_{0z} and H_{0z} are the initial values of the electric and magnetic fields at the boundaries, respectively, and $\beta = k_0$ is the propagation constant. For TE polarisation, the upper condition applies, while the reduced one is for TM polarisation. When the electric bounds field is a private mode, the border stays precisely not reflective.

3.5 Methods of computing

In FEM, a mathematical analysis process, the subdomains containing many unknown features are represented by subdomains and these unfamiliar functions simply interpolating. The COMSOL software solves the partial equations involved in computing, which use the finite-element method. By creating a range of physical equations and associated resolvers, the COMSOL can solve complicated physical issues which are interconnected. The distribution of materials and their EM characteristics are required parameters for COMSOL simulation. The material distribution and its EM characteristics are the parameters needed for simulation in COMSOL. The parameters which are required for simulation in COMSOL is the material distribution and their EM properties.

Finite-Element Analysis of Photonic Crystal Cavities in time and frequency domains :

A. Time domain

Considering an external current density J and with the help of Helmholtz equation the TE and TM fields are compactly described by the, as follows

$$-s \frac{q}{c^2} \frac{\partial \Phi}{\partial t^2} + s_y \frac{\partial}{\partial y} \left(p \frac{s_y}{s} \frac{\partial \Phi}{\partial y} \right) + s_y \frac{\partial}{\partial z} \left(p \frac{s_z}{s} \frac{\partial \Phi}{\partial z} \right) = \theta(J) \bullet \hat{a}_x \quad (3.13)$$

Where C : the speed of light in free space;

J : the density of current (external excitation);

$\Phi = E_x, p = 1, q = n^2$ and $\theta = -\mu_0 \frac{\partial}{\partial t}$ for TE modes;

$\Phi = H_x, p = \frac{1}{n^2}, q = 1$ and $\theta = -\nabla \times \frac{1}{n^2}$ for TM modes;

n : the refractive index;

μ_0 : the free-space permeability and

\hat{a}_x : the unit vector in the x direction.

s, s_y and s_z are the parameters related to absorbing the boundary conditions of the perfectly matched layers (PML) type, and the parameter s is given by

Φ	p	q	θ
E_x	1	n^2	$\theta = -\mu_0 \frac{\partial}{\partial t}$
H_x	$\frac{1}{n^2}$	1	$-\nabla \times \frac{1}{n^2}$

Table 3.1: Definition of symbols in wave equation

s_y	s_z	PML's location
1	s	Perpendicular to y axis
s	1	perpendicular to z axis
1	1	on the corners

Table 3.2: values of s_y and s_z

$$s = \begin{cases} 1 - j \frac{3c}{2\omega_0 n d} \left(\frac{\rho}{d}\right)^2 \ln \frac{1}{R} & \text{in PML regions} \\ 1 & \text{in other regions} \end{cases} \quad (3.14)$$

where $j = \sqrt{-1}$,

ω_0 : the angular frequency,

d : the thickness of the PML layer;

ρ : the distance from the beginning of PML and

R : the theoretical reflection coefficient.

The other parameters like s_y and s_z take the values as described in the table.

Since ω_0 : considered as the center frequency of the wave and the field is given by

$$\Phi = \phi(y, z, t) \exp(j\omega_0 t) \quad (3.15)$$

where $\phi(y, z, t)$ represents the wave's slowly varying envelope and the current density J is given in the same way i.e., $J = V(y, z, t) \exp(j\omega_0 t)$, with $V(y, z, t)$ being the slowly varying current density. Substituting these expressions into eqn(3.13), dividing the spatial domains into curvilinear triangular elements and then by applying the conventional FEM procedure we can obtain the following equation for slowly varying envelope.

$$-\frac{1}{c^2} [M] \frac{\partial^2 \{\phi\}}{\partial t^2} - 2j \frac{\omega_0}{c^2} [M] \frac{\partial \{\phi\}}{\partial t} + \left([k] + \frac{\omega_0^2}{c^2} [M] \right) \{\phi\} = \{f\} \quad (3.16)$$

where $[m]$ $[k]$ are matrices and they are represented as

$$[M] = \sum_e \iint_e s_q \{N\} \{N\}^T dydz \quad (3.17)$$

$$[K] = \sum_e \iint_e \left[-p \frac{s_y^2}{s} \frac{\partial \{N\}}{\partial y} \frac{\partial \{N\}^T}{\partial y} - p \frac{s_z^2}{s} \frac{\partial \{N\}}{\partial z} \frac{\partial \{N\}^T}{\partial z} \right] dydz \quad (3.18)$$

where N : the shape function vector,

T denotes a transpose,

\sum_e extends over all different elements and

f represents the external stimulation and is given by the following equation. The vector V is nonzero only at the positions which are corresponding to the nodal points, where it is applied.

$$\{f\} = \begin{cases} - \int \mu_0 \{N\} \left(j\omega_0 \{V_x\} + \frac{\partial \{V_x\}}{dt} \right) dydz & \text{for TE modes} \\ - \int \{N\} \left(\nabla \times \frac{1}{n^2} \{V\} \right)_x dydz & \text{for TM modes} \end{cases} \quad (3.19)$$

Isoparametric curvilinear six-node elements are used for the spatial discretization. The time variable discretization is based on the Newmark – Beta formulation, we obtain the following

$$\frac{d^2 \{\phi\}}{dt^2} = \frac{1}{\Delta t^2} [\{\phi\}_{i+1} - 2\{\phi\}_i + \{\phi\}_{i-1}] \quad (3.20)$$

$$\frac{d\{\phi\}}{dt} = \frac{1}{\Delta 2t} [\{\phi\}_{i+1} - \{\phi\}_{i-1}] \quad (3.21)$$

$$\{\phi\} = [\beta \{\phi\}_{i+1} + (1 - 2\beta) \{\phi\}_i + \beta \{\phi\}_{i-1}] \quad (3.22)$$

where Δt is the time step, the subscripts (i-1)th, ith and the (i+1)th time steps respectively, and $\beta (0 \leq \beta \leq 1.0)$ controls the stability of the method. The marching relation is given by

$$A = B + C \quad (3.23)$$

Where

$$A = \left[-\frac{1}{c^2 \Delta t^2} [M] - j \frac{\omega_0}{c^2 \Delta t} [M] + \beta \left([K] + \frac{\omega_0^2}{c^2} [M] \right) \right] \{\phi\}_{i+1}$$

$$B = \left[-\frac{2}{c^2 \Delta t} [M] - (1 - 2\beta) \left([K] + \frac{\omega_0^2}{c^2} [M] \right) \right] \{\phi\}_i$$

$$C = \left[\frac{1}{c^2 \Delta t^2} [M] - j \frac{\omega_0}{c^2 \Delta t} [M] - \beta \left([K] + \frac{\omega_0^2}{c^2} [M] \right) \right] \{\phi\}_{i-1} + \{f\}_i$$

The lower and upper triangle matrix (LU) decomposition is determined by the above equation during the first phase and by forward and reverse replacement in each phase for the following sector. The initial conditions are $\{\phi\}_1 = \{\phi\}_0 = 0$.

The Q factor is an significant cavity parameter and informs us how many oscillations the energy falls in $e^{-2\pi}$ its original value. We can obtain the Q factor from energy time variation as follows

$$Q = 2\pi \frac{|U_t|^2}{|U_t|^2 - |U_{t+T}|^2} \quad (3.24)$$

where U_t : the energy at an arbitrary time position,
 U_{t+T} : the energy after one cycle and
the cycle T corresponds to the resonant frequency.
Another convenient method to compute Q is

$$Q = \frac{\omega_0(t_1 - t_0)}{2 \ln \left(\frac{\phi_1}{\phi_0} \right)} \quad (3.25)$$

where ϕ_0 and ϕ_1 : Amplitudes at arbitrary moments of electromagnetic areas t_0 and t_1 , respectively.

B. Frequency-Domain Analysis : The frequency-domain scalar equation governing the transverse TE and TM modes, over a spatial domain y-z including PMLs, free of charges ($J=0$), is obtained with the factor $j\omega_0$ by replacing the operator $\frac{\partial}{\partial t}$ as follows :

$$sq \frac{\omega_0^2}{c^2} \phi + s_y \frac{\partial}{\partial y} \left(p \frac{s_y}{s} \frac{\partial \phi}{\partial y} \right) + s_z \frac{\partial}{\partial z} \left(p \frac{s_z}{s} \frac{\partial \phi}{\partial z} \right) = 0. \quad (3.26)$$

Where C is the speed of light in free space;
J is the density of current (external excitation);
 $\Phi = E_x, p = 1, q = n^2$ and $\theta = -\mu_0 \frac{\partial}{\partial t}$ for TE modes;
 $\Phi = H_x, p = \frac{1}{n^2}, q = 1$ and $\theta = -\nabla \times \frac{1}{n^2}$ for TM modes;
n is the refractive index; μ_0 is the free-space permeability; and \hat{a}_x is the unit vector

in the x direction. s , s_y and s_z are the parameters related to absorbing the boundary conditions of the perfectly matched layers (PML) type. By solving the above equation further using Galerkin method we can obtain the below equations

$$[A]\phi = \left(\frac{\omega_0^2}{c}\right)^2 [B]\{\phi\} \quad (3.27)$$

where ϕ is the vector field and the matrices $[A]$ and $[B]$ are given by

$$[A] = \sum_e \iint_e \left[p \frac{s_y^2}{s} \frac{\partial\{N\}}{\partial y} \frac{\partial\{N\}^T}{\partial y} + p \frac{s_z^2}{s} \frac{\partial\{N\}}{\partial z} \frac{\partial\{N\}^T}{\partial z} \right] dydz \quad (3.28)$$

$$[B] = \sum_e \iint_e sq\{N\}\{N\}^T dydz \quad (3.29)$$

The subspace iteration method is used to solve the resulting sparse complex eigenvalues system efficiently. There by we obtain the field resolution and the complex resonant frequency of the field ω_0 . The Q factor of the mode which is associated with the complex frequency ω_0 is given by

$$Q = Re \frac{[\omega_0]}{2Im[\omega_0]} \quad (3.30)$$

where Re and Im stands for the real and imaginary parts, respectively. The field of distribution is used to compute the modal area A as follows

$$A = \frac{\int n^2 |\phi|^2 dydz}{\max(n^2 |\phi|^2)} \quad (3.31)$$

where ϕ is E_x or H_x of the field.

When the EM wave energies flow inside or outside the PhCs, a port limit is used. Specific electromagnetic field patterns can be started and absorbed and S parameter measurement is supported. T spectrum for the PhCs will be calculated using the S21 parameters, that is,

$$S_{21} = \frac{\iint \vec{E} \cdot \vec{E}_2}{\iint \vec{E}_2 \cdot \vec{E}_2} \quad (3.32)$$

where \vec{E} is the electric field, which consists of both excitation as well as reflected field on port 1. The excitation field and the reflected field are calculated by using the eigenmode analysis on two ports i.e port 1 and port 2.

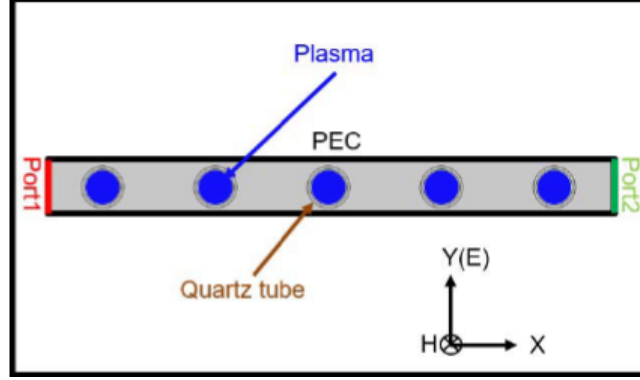


Figure 3.1: Schematic of 1-D PPCs which is to be designed.

3.6 Computational model of 1D plasma photonic crystal

The 1-D PPCs are formed from an array of five quartz tubes ($\epsilon_{ra} = 3.8$) of diameter $d = 15$ mm and a wall thickness of 1 mm. The lattice constant of this photonic crystal $a = 40$ mm. The quartz tubes are filled with the homogenous plasma and the background medium is air ($\epsilon_{rd} = 1$). The permittivity of the plasma is given by

$$\epsilon_{rp} = 1 - \frac{\omega_{pe}^2}{\omega^2} \left[\frac{1}{1 - i(\frac{v_m}{\omega})} \right] \quad (3.33)$$

where ω is the angular frequency of the incident EM wave and v_m is the electron neutral elastic collision frequency. ω_p is the plasma which is related to the plasma density n_e .

$$\omega_p = \sqrt{\frac{n_e e^2}{m_e \epsilon_0}} \quad (3.34)$$

where e is the electron charge, ϵ is the permittivity of vacuum, m_e is the electron mass.

By changing the frequency of the incident wave, plasma density and collision frequency the dielectric function of the plasma can be adjusted. The cutoff frequency is the frequency at which the dielectric constant of the plasma becomes zero. While performing the simulations the collision frequency is ignored because it has a very little effect on the position and width of the photonic bandgap.

3.7 Photonic Crystal filters

In order to transmit data through large distances while maintaining high data rates we need all optical communication networks. This network involves optical devices like optical demultiplexers, optical switches and optical filters etc. In order to filter out or remove noise and the unwanted signals from this communication channel optical filters are used. They are also used in WDM (Wavelength Division Multiplexing) in order to design demultiplexers in optical domain. The ability of the photonic crystals to control light even in ultrasmall (uncomparable) dimensions makes them suitable for design of optical filters.

There are two ways for realizing a filter. In the first method a defect layer is introduced into the PhC structure through which a PBG is generated so that it can be used as a filter. The other way of realizing a multichannel filter using the 1DPhC is by replacing the dielectric layers with superconducting PhC, defect layers are not introduced in these structures. In this work we will talking only about the first method in which a defect layer is introduced into the PhC. By using these two methods we will be developing two filters one is narrow band filter and the other is narrow transmission angle filter, the other filter which is based on 1D PhC is band rejection filter or reflection filter. These 1D PhC do not have complete bandgaps which makes them sensitive to the input wave's incident angle. But in the case of a 2D PhC structure the wavelength of resonance will be depending on the resonant ring's dimensions and as well as the resonant wavelength of the refractive index.

Chapter 4

Simulation & Results

4.1 Designing parameters

The designing parameters of the photonic crystal plays an important role as we are dealing with a very small component where minute changes in the structure or the properties will play a major role. Basic parameters like the length of the unit cell, beam width SiN film thickness, circular small radius, normalized special k, circular large radius, K vector in X direction, vacuum layer width, vacuum layer height, SiN reflective index. The conductivity of the crystal is kept zero to avoid the wave confinement on it.

name	expression	value	Description
L_cell	280[mm]	0.28m	unit cell length
w_beam	40[mm]	0.04m	beamwidth
$h_{nitride}$	40[mm]	0.04m	SiN film thickness
r_hole_small	14[mm]	0.14m	circular small radius
k_x_N	1	1	normalized special k
r_hole_large	15[mm]	0.015m	circular large radius.
k_x	$k_x_N * \pi / L_{cell}$	11.22 1/m	K vector in X direction.
w_air	$5 * w_{beam}$	0.2m	vaccum layer width
h_air	$5 * h_{nitride}$	0.2m	vaccume layer height
n_nitride	2.016	2.016	SiN reflective index

Table 4.1: Parameters used in the design of waveguide

4.2 Structure of the photonic crystal and simulations

The PPC which is designed is a periodic array of plasma in a rectangular shape with five holes made for insertion of plasma into it with periodic intervals. The electron density of this plasma is varied and the bandgaps for different electron densities is observed. The PEC is the limiting situation for the x-component of the interface electric field 0. The PEC limiting situation (except the port limit) is used at the limit of the simulation domain ; both link and correct borders are set in the port border for the simulation domain. The EM wave is excited from port 1 and the input power (P_{in}) is 1 W, and the amplitude of Y component of electric field (E_y) is 1.

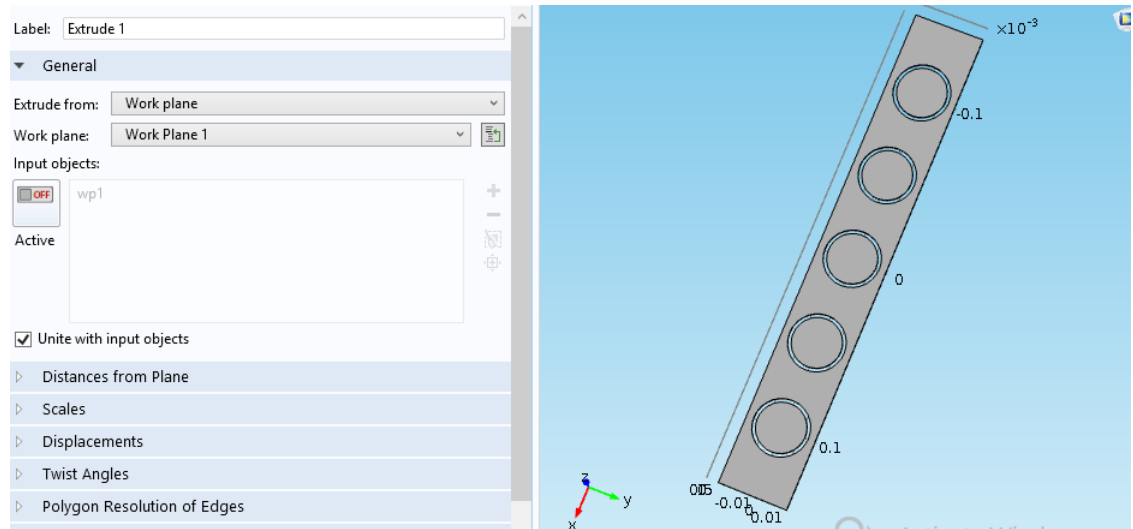


Figure 4.1: Structure of the photonic crystal designed in comsol with five quartz tubes filled with plasma.

When an electromagnetic wave is made to propagate through the above structure the electromagnetic wave interacts with the plasma inserted in the photonic crystal at particular eigen frequencies depending on the plasma density. Different modes are observed for that particular eigen frequency and the confinement which is obtained on the photonic crystal and the convergence plot which indicates the error value is also plotted. The polarization in the modes and the quasi TE and TM modes were also represented in the following figures.

In the figure 4.2 when an electromagnetic wave is made to propagate through the above structure the electromagnetic wave interacts with the plasma inserted in the photonic crystal at an eigen frequency value of $3.4762E9+2.3651E9i$ (4) depending on the

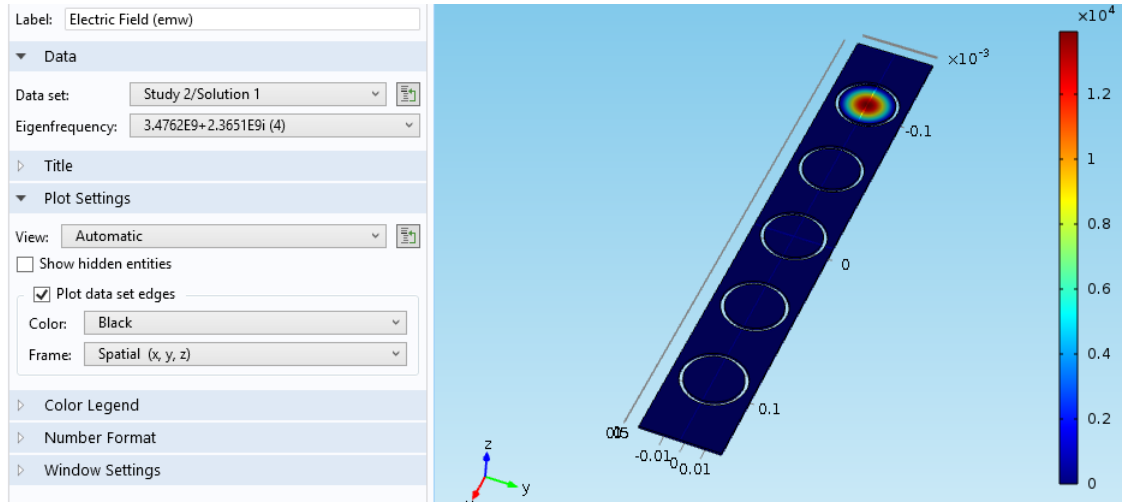


Figure 4.2: 1-D PPC at first eigen frequency.

plasma density.

In figure 4.3 when an electromagnetic wave is made to propagate through the above structure the electromagnetic wave interacts with the plasma inserted in the photonic crystal at an eigen frequency value of $3.4762E9+2.3651E9i$ (3) depending on the plasma density.

In figure 4.4 when an electromagnetic wave is made to propagate through the above structure the electromagnetic wave interacts with the plasma inserted in the photonic crystal at an eigen frequency value of $3.4762E9+2.3651E9i$ (1) depending on the plasma density.

In figure 4.5 when an electromagnetic wave is made to propagate through the above structure the electromagnetic wave interacts with the plasma inserted in the photonic crystal at an eigen frequency value of $3.4762E9+2.3651E9i$ (2) depending on the plasma density.

In figure 4.6 when an electromagnetic wave is made to propagate through the above structure the electromagnetic wave interacts with the plasma inserted in the photonic crystal at an eigen frequency value of $3.4762E9+2.3651E9i$ (5) depending on the plasma density.

The convergence plot which is in the above figure 4.2 shows that the error value in the confinement of the wave is decreasing with the increase in number of iterations.

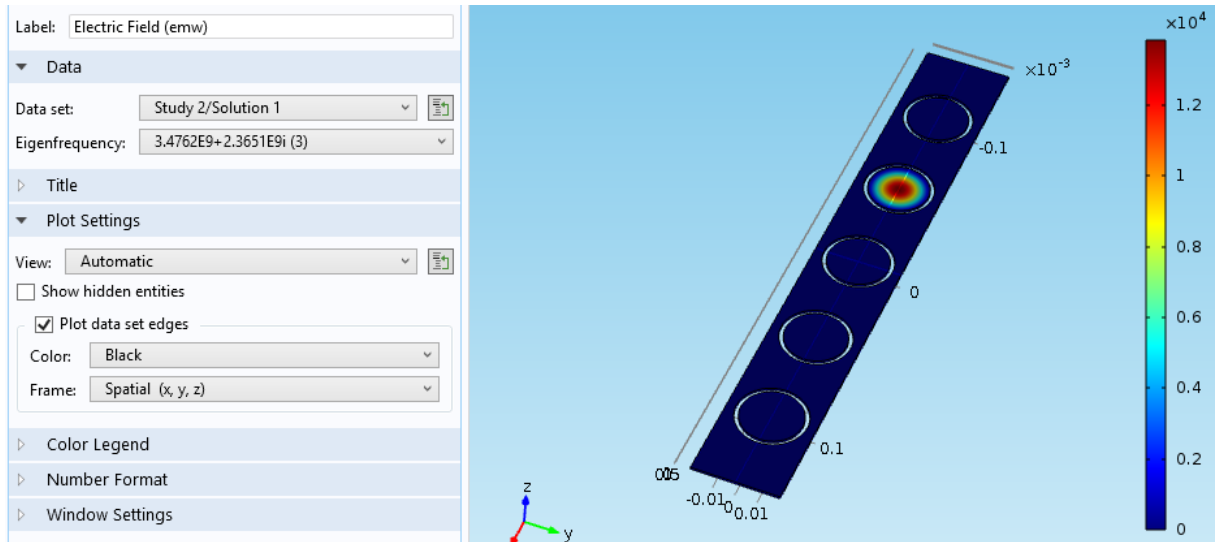


Figure 4.3: 1-D PPC at second eigen frequency.

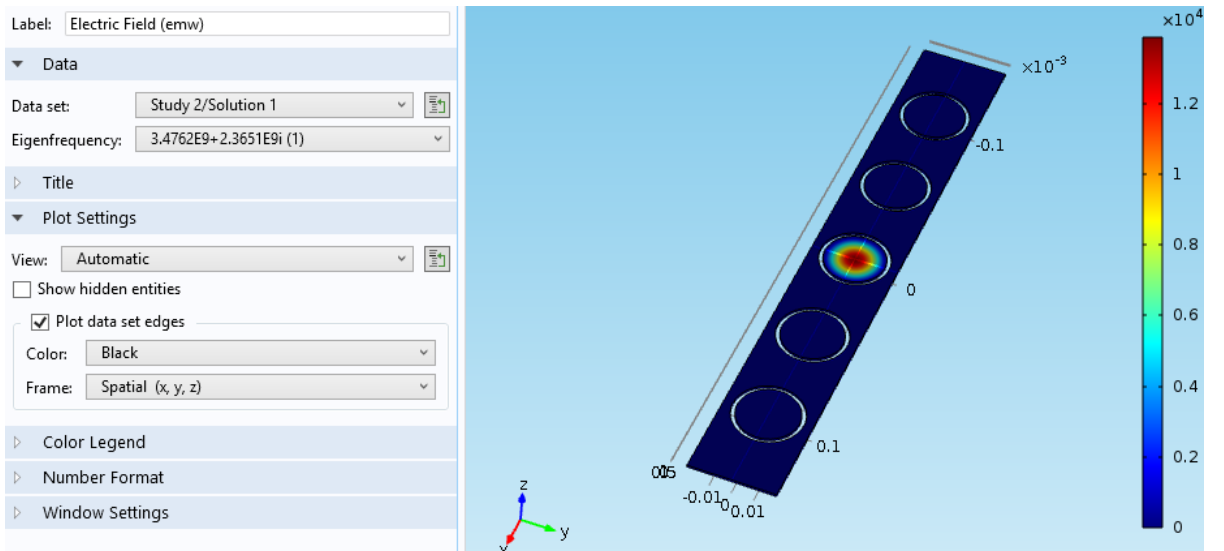


Figure 4.4: 1-D PPC at third eigen frequency.

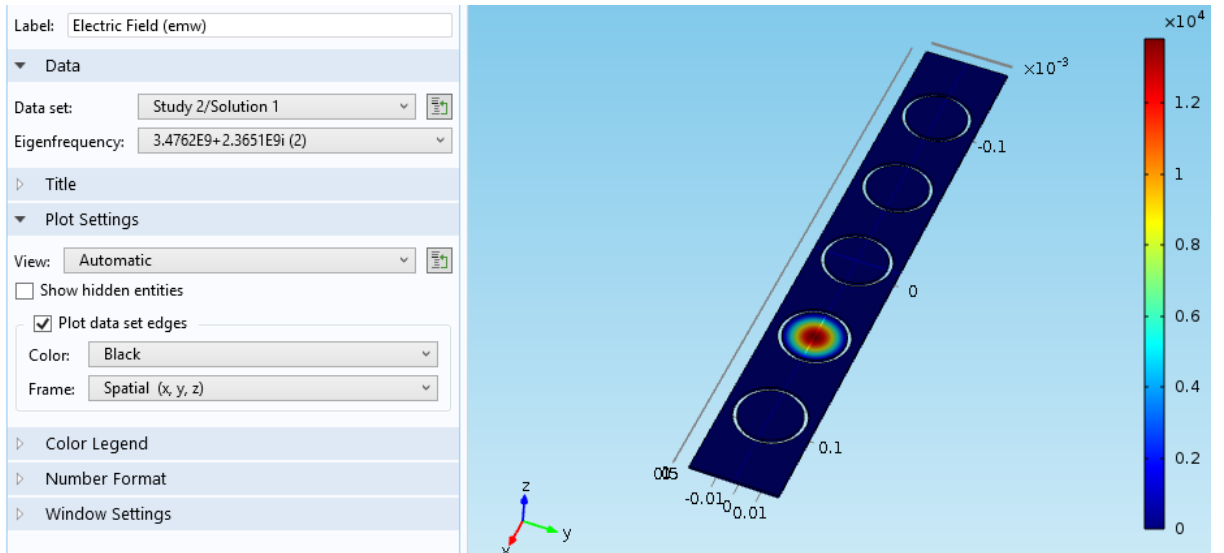


Figure 4.5: 1-D PPC at fourth eigen frequency

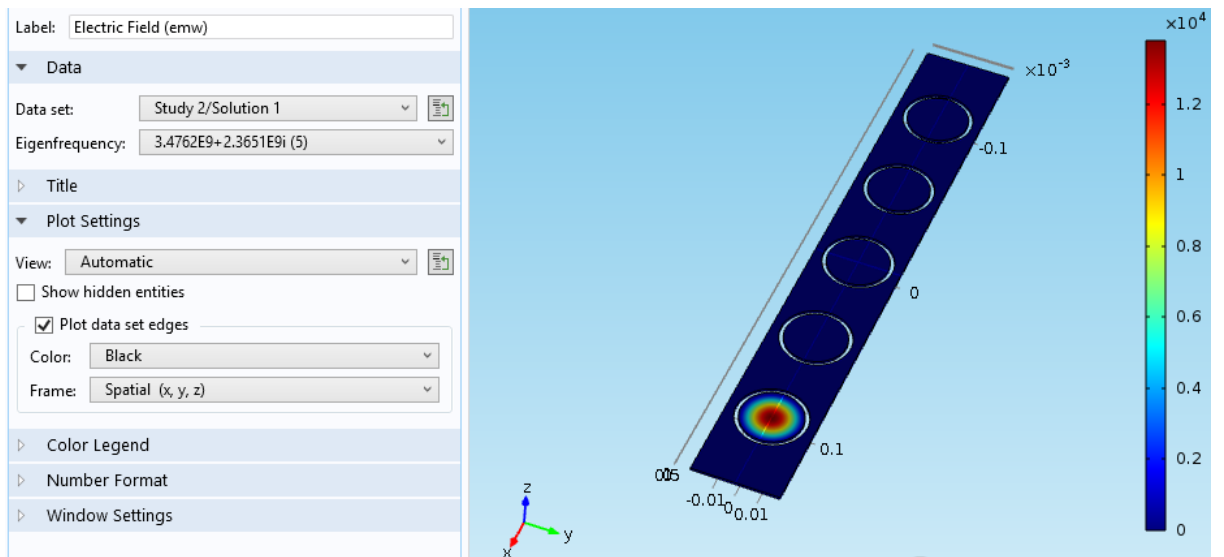


Figure 4.6: 1-D PPC at fifth eigen frequency.

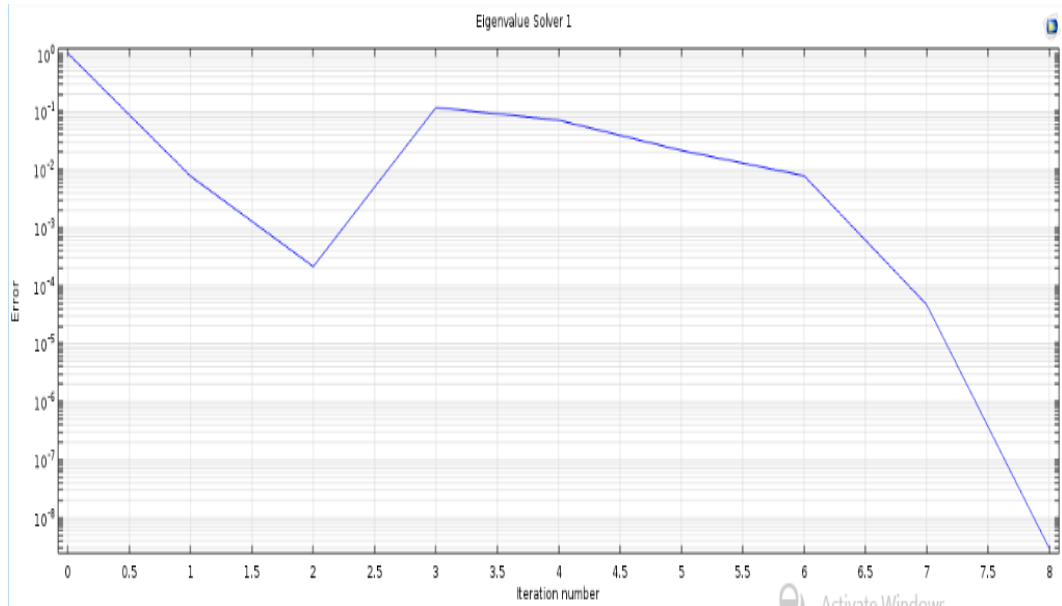


Figure 4.7: convergence plot.

4.3 Quasi modes

Energy confined in both the transverse direction i.e for both transverse electric and transverse magnetic. Modes in channel waveguides like rectangular waveguides contain all six field components $(E_x, E_y, E_z, H_x, H_y, H_z)$. Energy is strictly confined to two areas and free to propagate in the third axis. There is no way to justify the cancelling any of these terms in Maxwell equations. TE and TM modes do not exist in channel waveguides only hybride modes exist. The modes are usually strongly linearly polarized and often components can be ignored to simplify analysis with little loss in accuracy some approximations are made and the modes were called as quasi TE and quasi TM modes. The higher the order of the mode the more significant is the coupling. Most of the waveguides support only single order mode. Energy is confined to only one transverse direction in a slab waveguide and it is free to spread out in other transverse direction. Propagation with in a slab can be restricted to a single direction without rigorously decouple into two distinct modes. E_z mode, for E_z mode the electric field is always tangential to metal interfaces and whatever the problems exist they were only in the modeling of the metallic structure. H_z mode, for H_z mode the electric field can be polarized perpendicular to the metal interfaces. This is difficult and is best placed in the surface of contact with metals with outermost areas.

In fiure 4.8 when an electromagnetic wave is made to propagate through the above

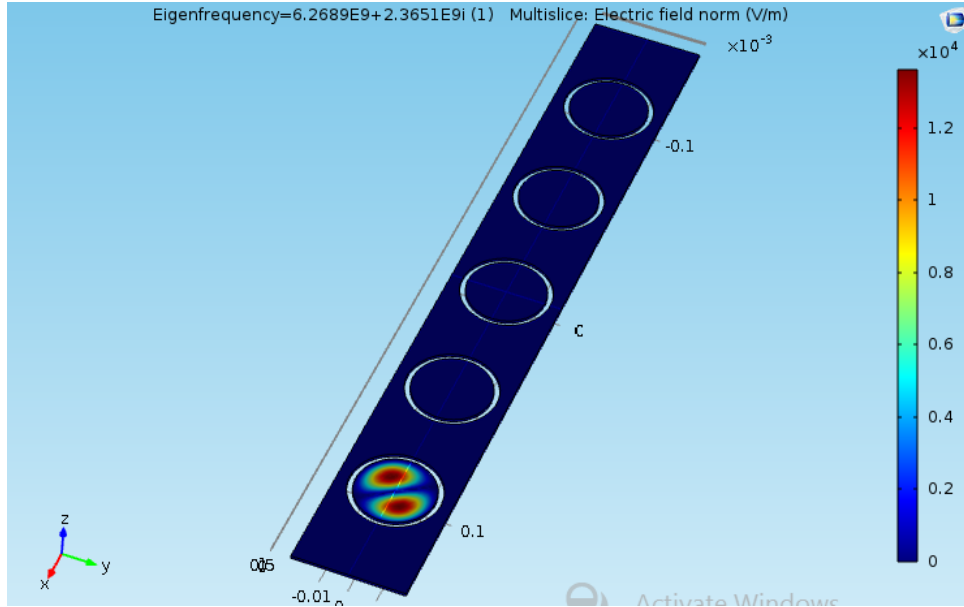


Figure 4.8: 1-D PPC at sixth eigen frequency.

structure the electromagnetic wave interacts with the plasma inserted in the photonic crystal at an eigen frequency value of $6.2689E9 + 2.3651E9i$ (1) depending on the plasma density.

In figure 4.9 when an electromagnetic wave is made to propagate through the above structure the electromagnetic wave interacts with the plasma inserted in the photonic crystal at an eigen frequency value of $6.2689E9 + 2.3651E9i$ (2) depending on the plasma density.

In figure 4.10 when an electromagnetic wave is made to propagate through the above structure the electromagnetic wave interacts with the plasma inserted in the photonic crystal at an eigen frequency value of $6.2689E9 + 2.3651E9i$ (3) depending on the plasma density.

In figure 4.11 when an electromagnetic wave is made to propagate through the above structure the electromagnetic wave interacts with the plasma inserted in the photonic crystal at an eigen frequency value of $6.2689E9 + 2.3651E9i$ (4) depending on the plasma density.

In figure 4.12 when an electromagnetic wave is made to propagate through the above structure the electromagnetic wave interacts with the plasma inserted in the photonic crystal at an eigen frequency value of $6.2689E9 + 2.3651E9i$ (5) depending on the plasma density.

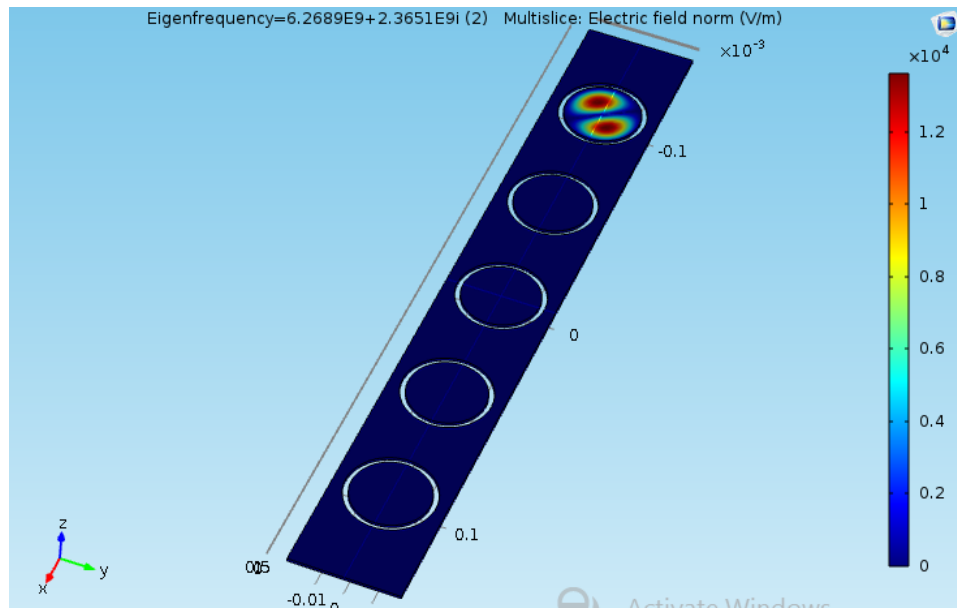


Figure 4.9: 1-D PPC at seventh eigen frequency.

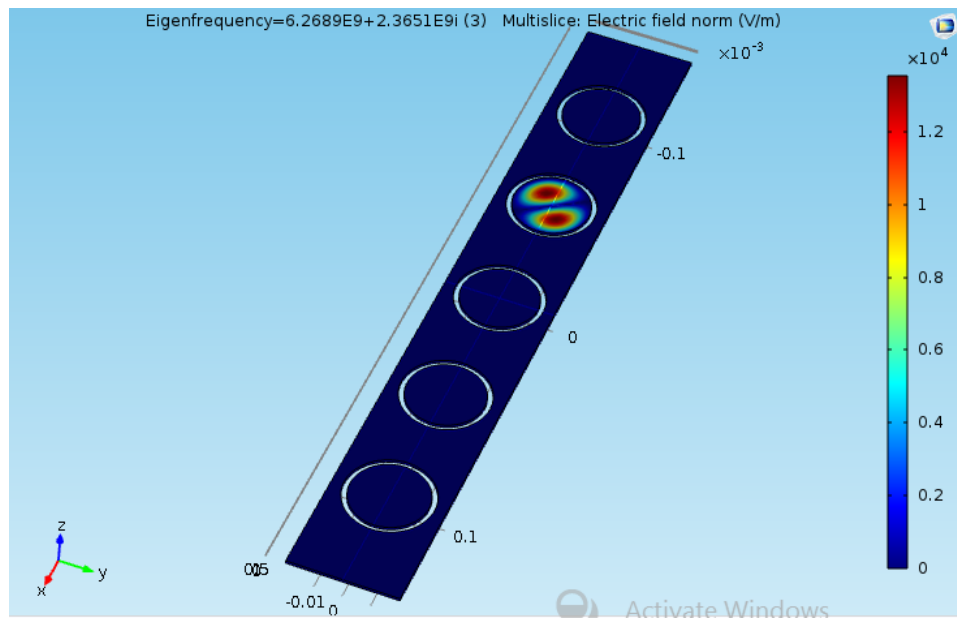


Figure 4.10: 1-D PPC at eighth eigen frequency.

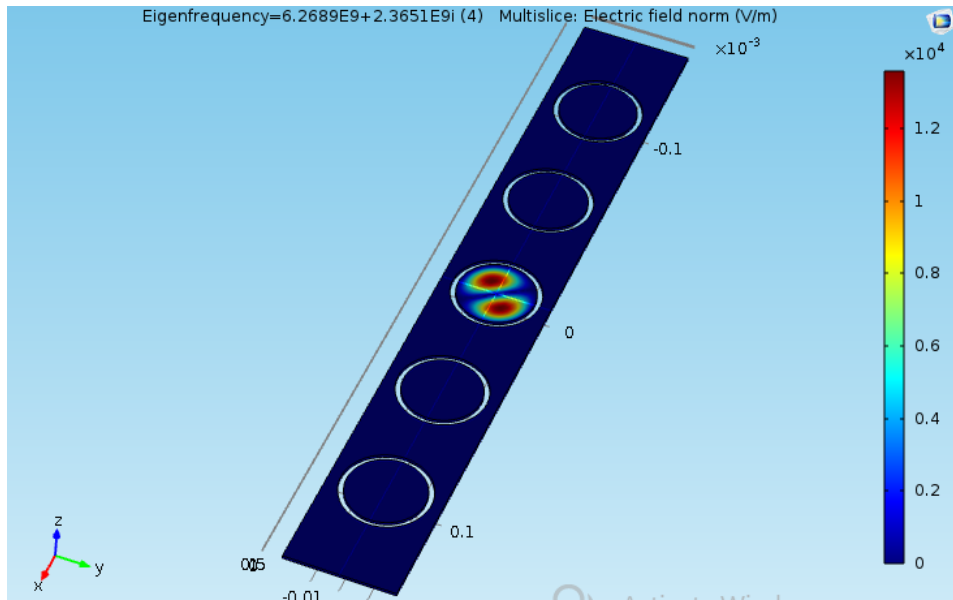


Figure 4.11: 1-D PPC at ninth eigen frequency.

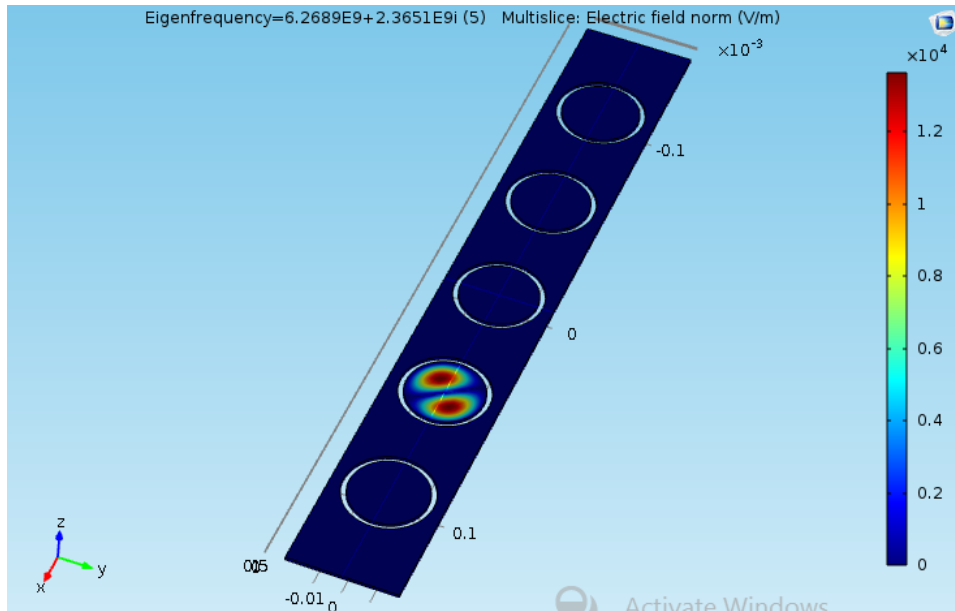


Figure 4.12: 1-D PPC at tenth eigen frequency.

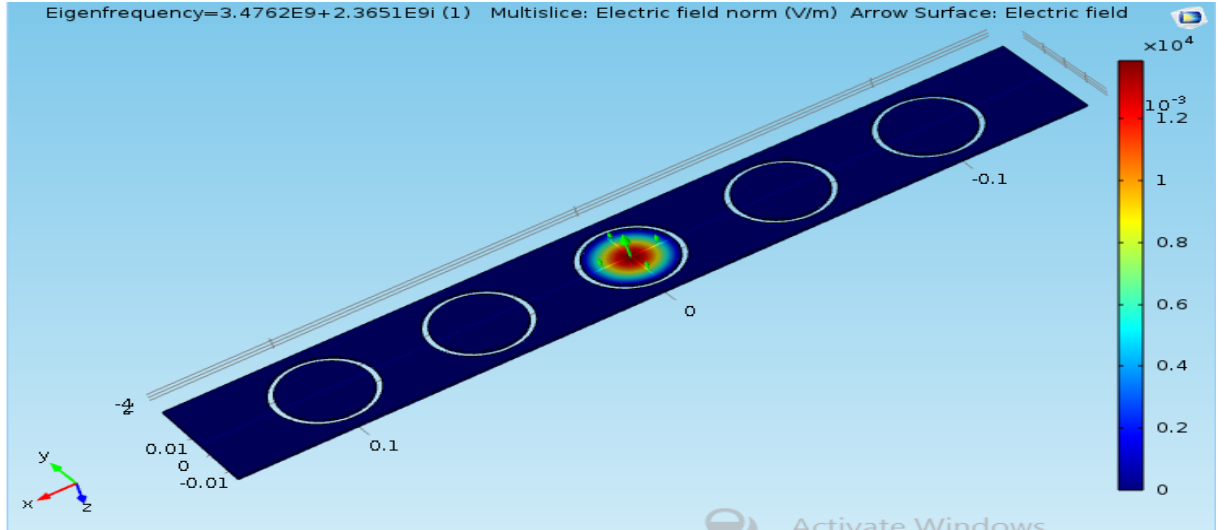


Figure 4.13: 1-D PPC at first eigen frequency with polarization.

In figure 4.9 when an electromagnetic wave is made to propagate through the above structure the electromagnetic wave interacts with the plasma inserted in the photonic crystal at an eigen frequency value of $3.4762E9+2.3651E9i$ (1) depending on the plasma density.

In figure 4.14 when an electromagnetic wave is made to propagate through the above structure the electromagnetic wave interacts with the plasma inserted in the photonic crystal at an eigen frequency value of $3.4762E9+2.3651E9i$ (2) depending on the plasma density.

In figure 4.15 when an electromagnetic wave is made to propagate through the above structure the electromagnetic wave interacts with the plasma inserted in the photonic crystal at an eigen frequency value of $3.4762E9+2.3651E9i$ (3) depending on the plasma density.

In figure 4.16 when an electromagnetic wave is made to propagate through the above structure the electromagnetic wave interacts with the plasma inserted in the photonic crystal at an eigen frequency value of $3.4762E9+2.3651E9i$ (4) depending on the plasma density.

In figure 4.17 when an electromagnetic wave is made to propagate through the above structure the electromagnetic wave interacts with the plasma inserted in the photonic crystal at an eigen frequency value of $3.4762E9+2.3651E9i$ (5) depending on the plasma density.

In figure 4.18 when an electromagnetic wave is made to propagate through the above

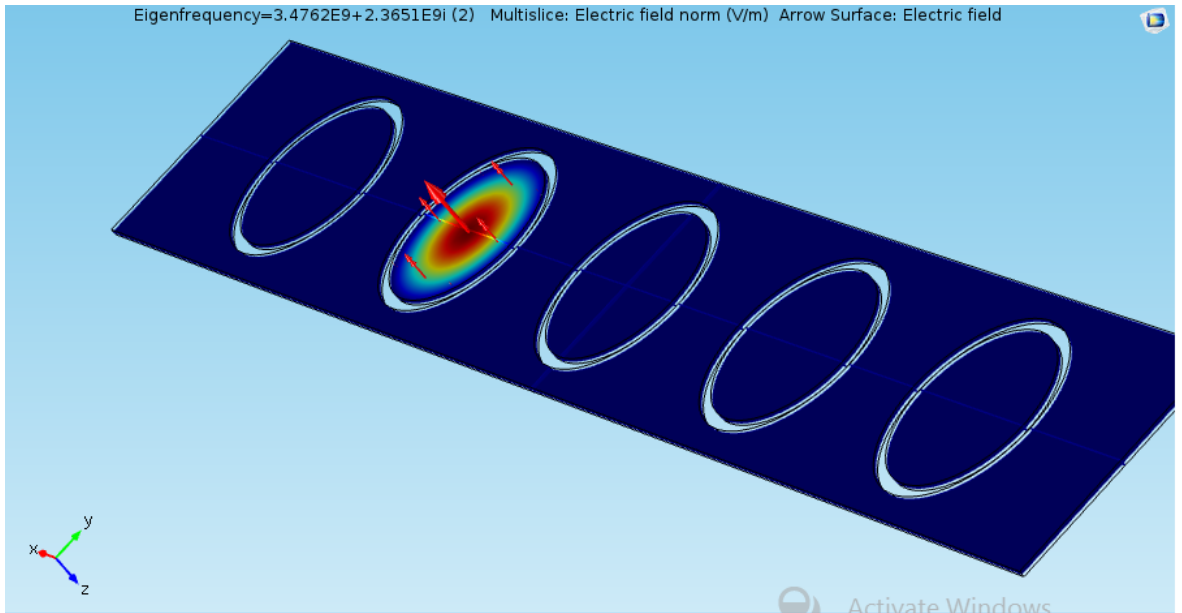


Figure 4.14: 1-D PPC at second eigen frequency with polarization.

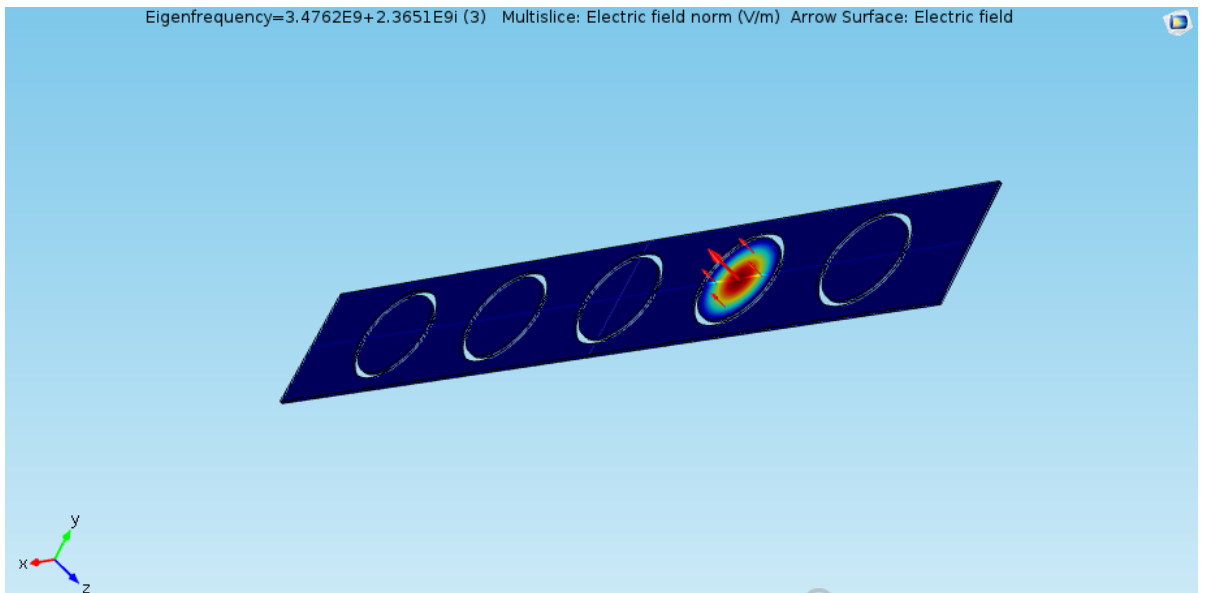


Figure 4.15: 1-D PPC at third eigen frequency with polarization.

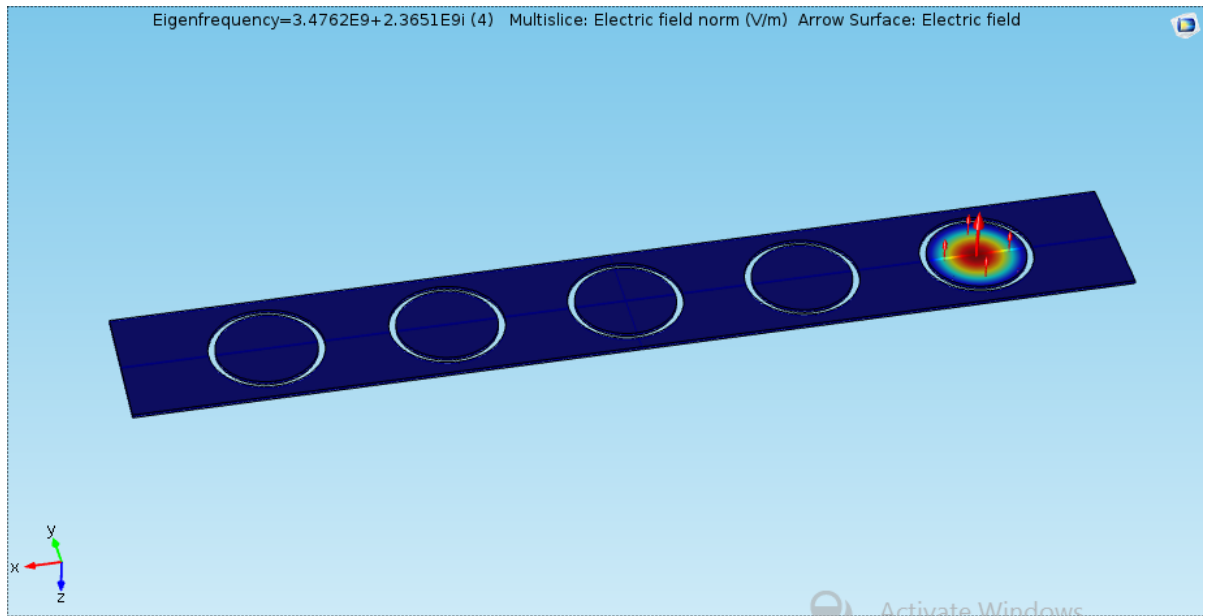


Figure 4.16: 1-D PPC at fourth eigen frequency with polariztion.

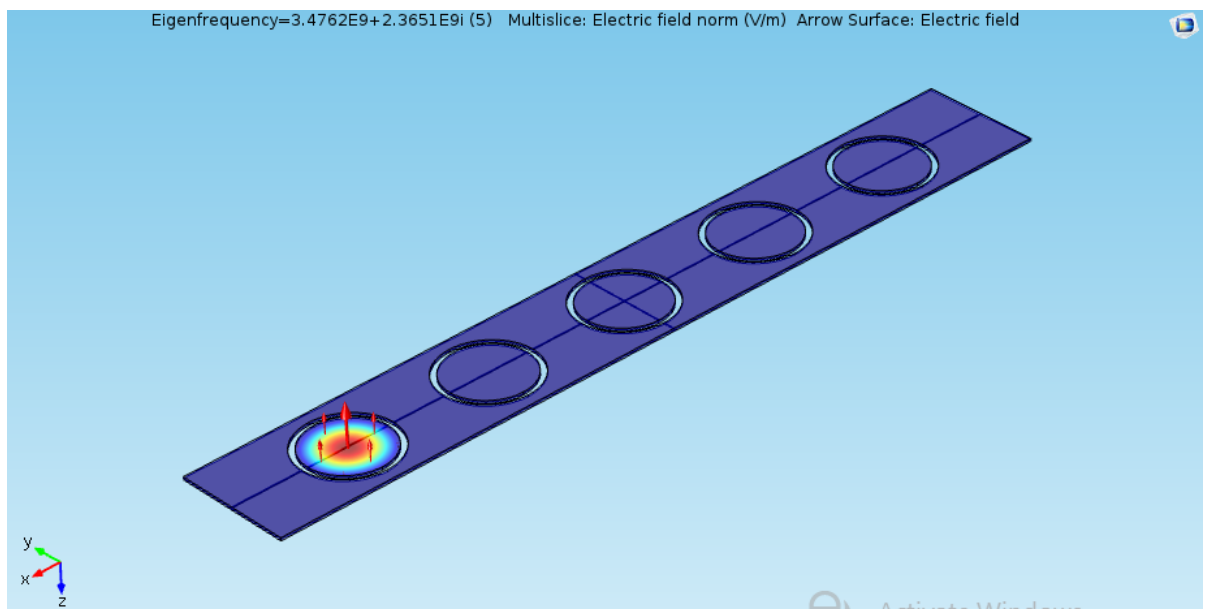


Figure 4.17: 1-D PPC at fifth eigen frequency with polariztion.

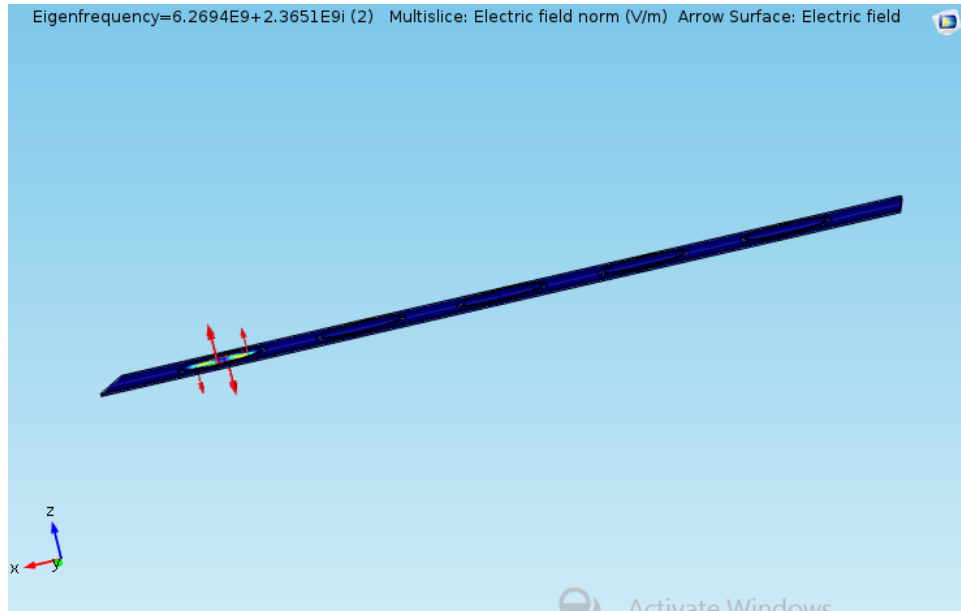


Figure 4.18: 1-D PPC at sixth eigen frequency with polarization.

structure the electromagnetic wave interacts with the plasma inserted in the photonic crystal at an eigen frequency value of $6.2694+2.3651E9i$ (1) depending on the plasma density.

In figure 4.19 when an electromagnetic wave is made to propagate through the above structure the electromagnetic wave interacts with the plasma inserted in the photonic crystal at an eigen frequency value of $6.2694+2.3651E9i$ (2) depending on the plasma density.

In figure 4.20 when an electromagnetic wave is made to propagate through the above structure the electromagnetic wave interacts with the plasma inserted in the photonic crystal at an eigen frequency value of $6.2694+2.3651E9i$ (3) depending on the plasma density.

In figure 4.21 when an electromagnetic wave is made to propagate through the above structure the electromagnetic wave interacts with the plasma inserted in the photonic crystal at an eigen frequency value of $6.2694+2.3651E9i$ (4) depending on the plasma density.

In figure 4.22 when an electromagnetic wave is made to propagate through the above structure the electromagnetic wave interacts with the plasma inserted in the photonic crystal at an eigen frequency value of $6.2694+2.3651E9i$ (5) depending on the plasma density.

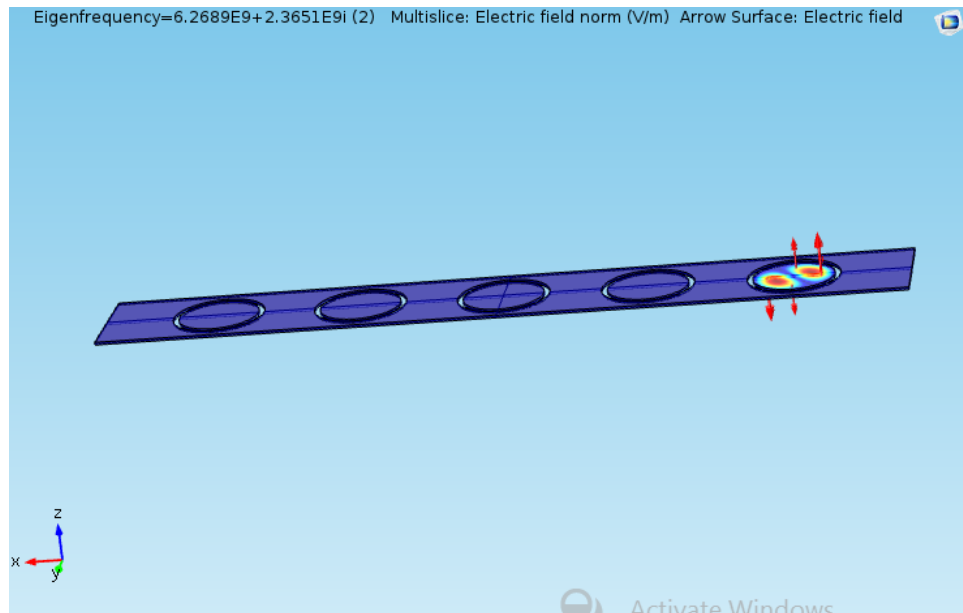


Figure 4.19: 1-D PPC at seventh eigen frequency with polarization.

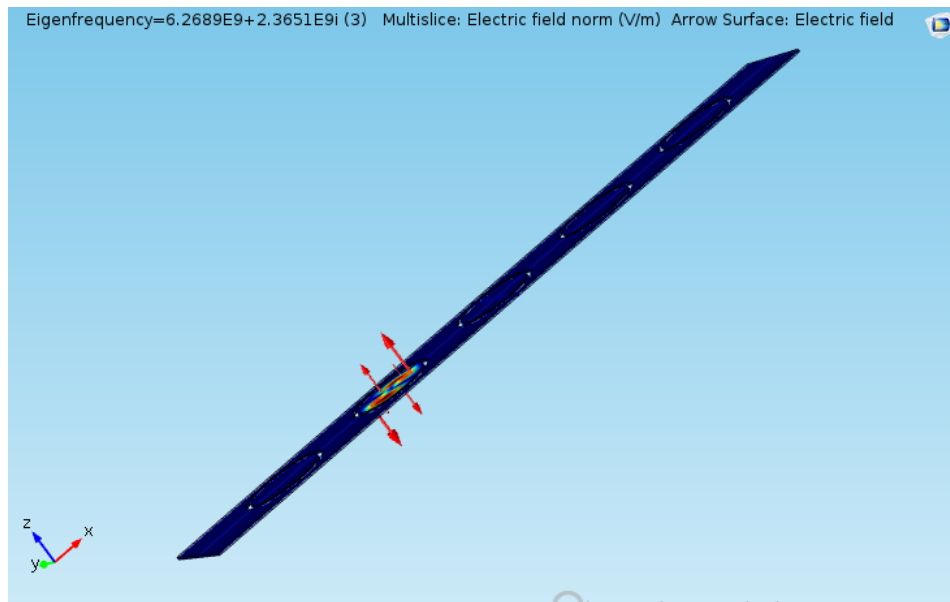


Figure 4.20: 1-D PPC at eighth eigen frequency with polarization.

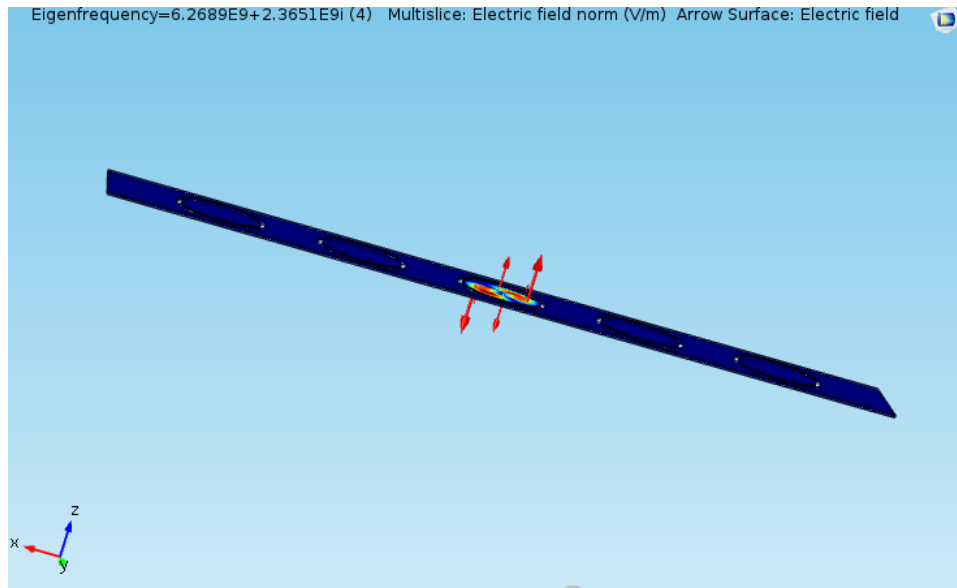


Figure 4.21: 1-D PPC at ninth eigen frequency with polarization.

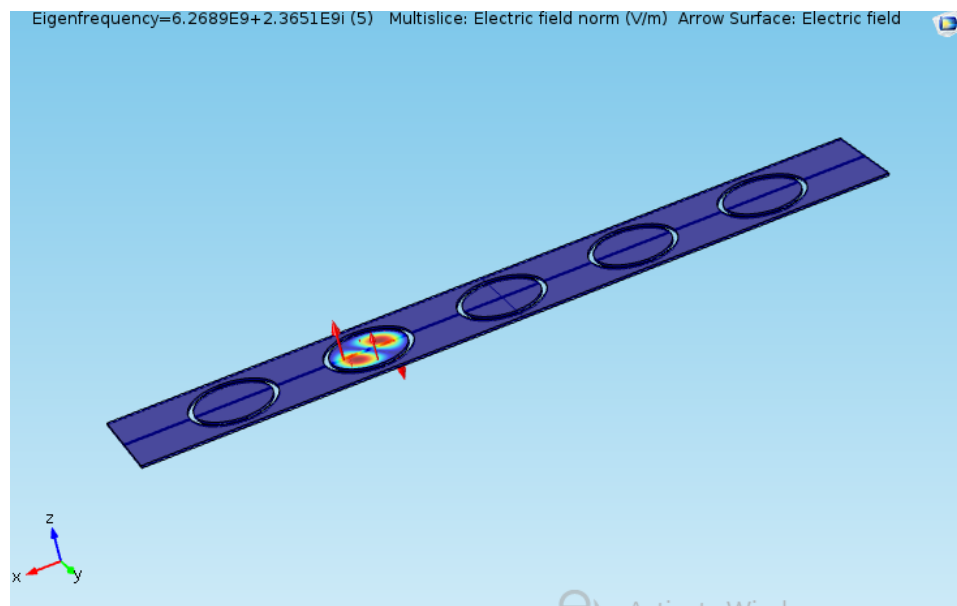


Figure 4.22: 1-D PPC at tenth eigen frequency with polarization.

4.4 Variations in the permittivity of the plasma photonic crystal

From the two equations mentioned below it can be seen that the dielectric function of the plasma can be varied with variations in the frequency of the incident wave, plasma density and collision frequency. The cutoff frequency is the frequency at which the dielectric constant of the plasma ϵ_{rp} becomes zero. The collision frequency is ignored during the simulation because its effect is very small on the width and position of the bandgap.

$$\epsilon_{rp} = 1 - \frac{\omega_{pe}^2}{\omega^2} \left[\frac{1}{1 - i\left(\frac{v_m}{\omega}\right)} \right] \quad (4.1)$$

ω is angular frequency of the incident EM wave and v_m is the electron neutral elastic collision frequency. ω_p is the plasma which is related to the plasma density n_e .

$$\omega_p = \sqrt{\frac{n_e e^2}{m_e \epsilon_0}} \quad (4.2)$$

where e is the electron charge, ϵ is the permittivity of vacuum, m_e is the electron mass.

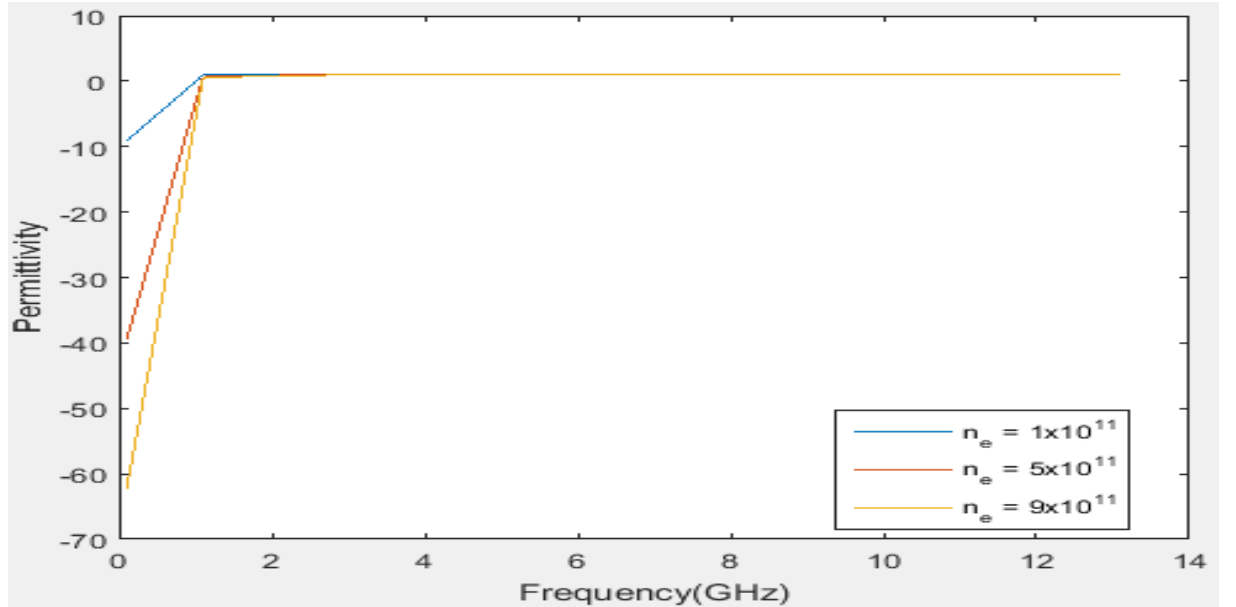


Figure 4.23: For various plasma densities the real components of the relative permittivity.

4.5 Bandgap variations for various plasma densities

The band gaps are observed clearly by using the frequency sweep function. In the figure 4.2.3, the relationship between dielectric constant, density of plasma, and frequency is shown. The plasma dielectric function is strictly linked to EM wave and plasma density incidents. The absorption coefficient of the plasma also shifts with the frequency of the incident wave. With respect to the cutoff frequency the dielectric constant is divided into positive and negative areas. For the area below the cutoff frequency, plasma permittivity is negative and some TE waves with certain frequencies can spread in the PPCs owing to the local resonance and sympathetic resonance connected with the surface plasmon wave. As the positive permittive region resides above cutoff frequency periodically dispersed on the plasma surface, some waves with certain frequencies can not spread in PPCs.

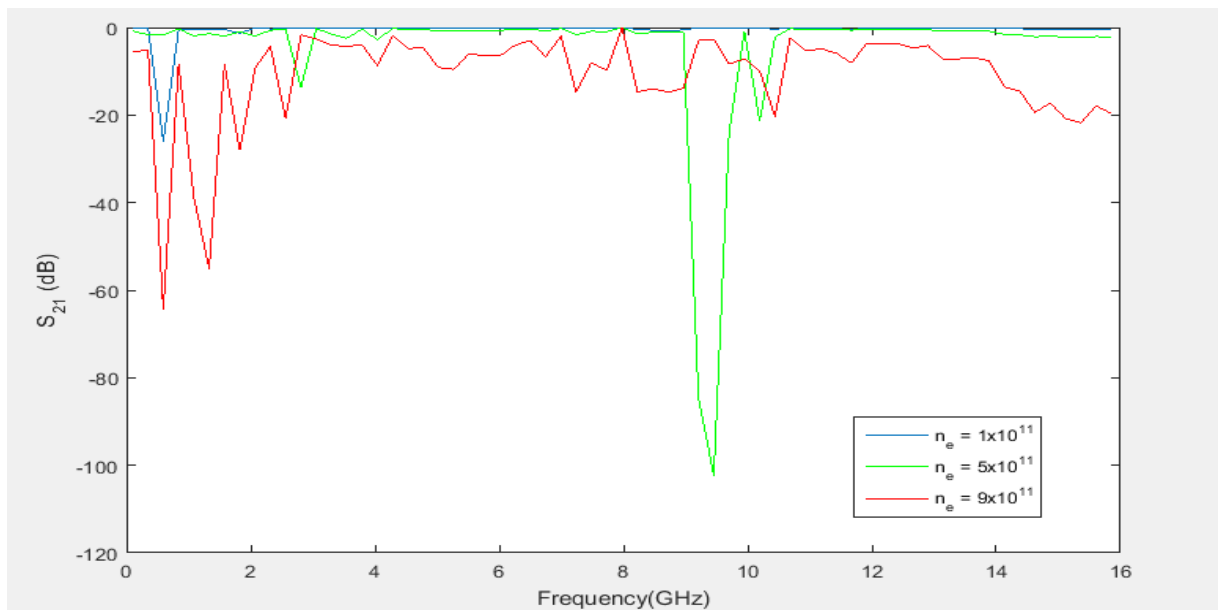


Figure 4.24: For various plasma densities the simulated bandgap is given. Here the bandwidth of the filter depending on the frequency which it restricts from passing through the crystal is calculated around 1GHz for $n_e = 5 \times 10^{11}$

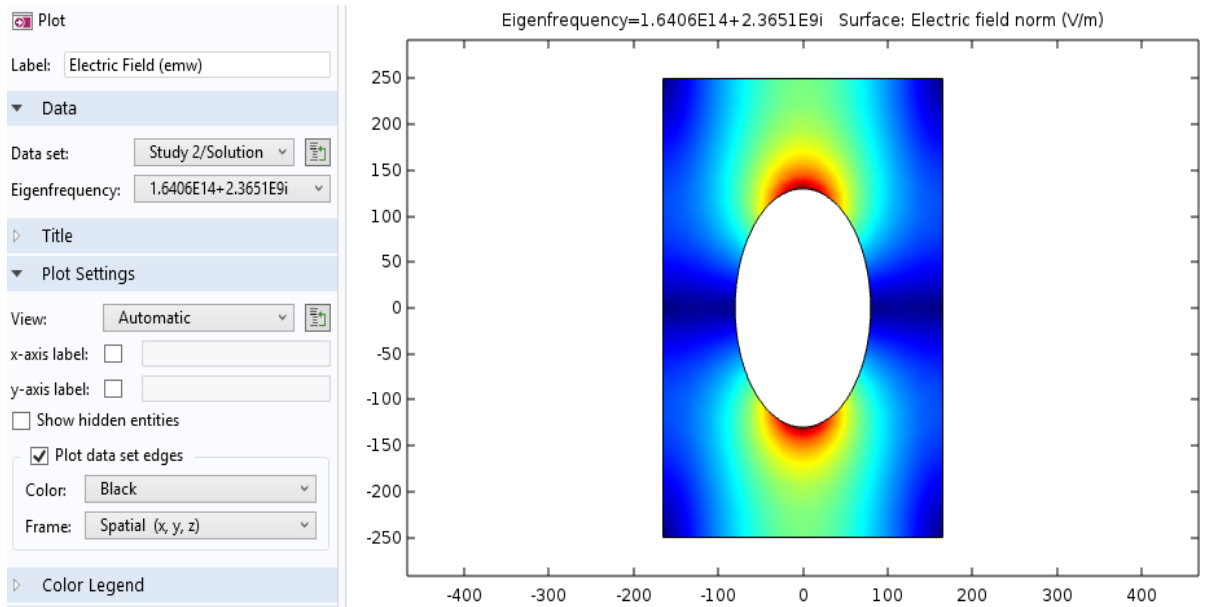


Figure 4.25: The photonic crystal structure when plasma is replaced with air . The above figure represents the photonic crystal with air inserted in it and it shows the characteristics of the EM wave propagating through it. The below graph shows how the wave is behaving in the frequency range of THz when it is incident on the photonic crystal which is shown above.

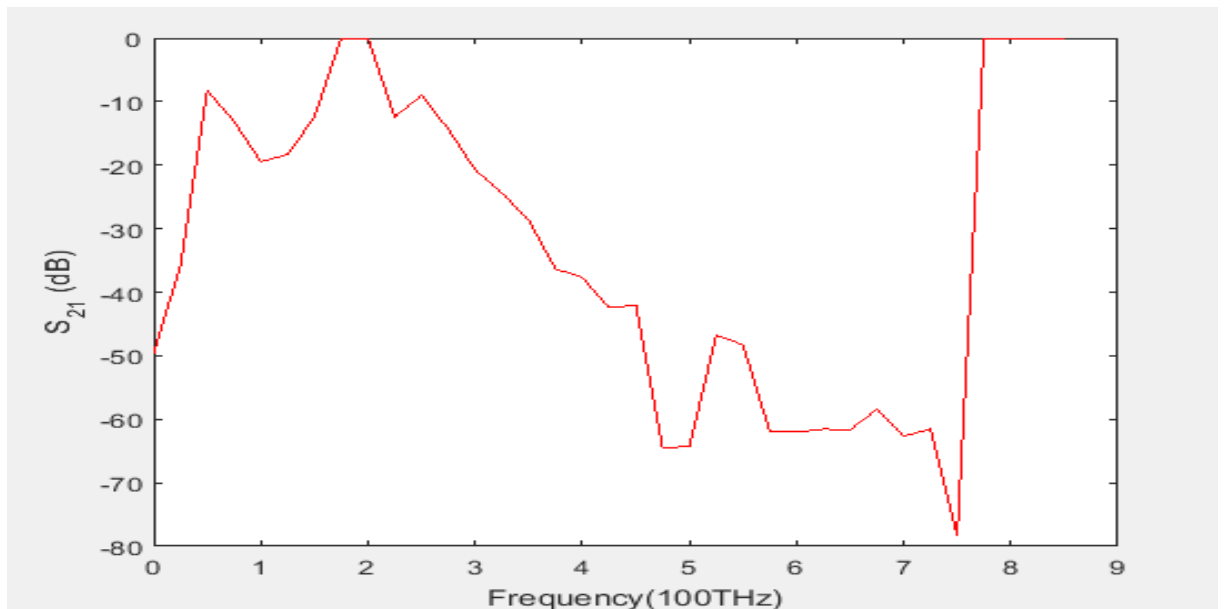


Figure 4.26: The photonic crystal structure when plasma is replaced with air.

Chapter 5

Conclusion and Future work

The 1-D PPC design used for the simulation model is quite useful for the reorganization of plasma density as well as for the monitoring of quartz release pipes. Transmission properties of the microwaves which are propagating through the 1-D PPCs are investigated. In the low-frequency regions the TE-mode adverse PBG structure 1-D PPCs were generated under circumstances below the cutoff region. Conditions above the cutoff region i.e. in the High Frequency Region where air acts as a high-dielectric constant slab and plasma placed as low-dielectric material in quartz tubes are associated with the periodic dispersion of the EM wave over the plasma surface. The variations in plasma density lead to modifications in the PBG composition through the effects of the Fano mode and the plasma surface wave. A number of Fano modes are constant to generate a broad passband in a cut off region and a number of sharp transmittance peaks in PBG will be made by surface modes. Due to the shift in the sign of the dielectric consolidation of the plasma, PBG created at circumstances near the cutoff frequency area can be removed. The results verify that all-PPC bandgaps are highly dependent on the density of plasma. The simulated PPC will serve as a point of reference in future to design comparable equipment and to further understand the interaction between EM waves and plasma and to enhance PhC research.

Currently this structure is analysed for the frequency range of around 16GHz, in future with required modifications performed on the structure as well as with the necessary changes made in the plasma density this PPC can be used to observe the wave behaviour at higher frequencies in order to extend the application of PPCs into the visible light region.

A photonic crystal is designed with air inserted in it and the characteristics of the

EM wave which is made to propagate through it are observed for a single section. The Photonic crystal which is shown shown is operating at a frequency value of 1.64×10^{14} when converted to wavelength it is around 1825 nanometers, further modifacations can be made to the PhC so that it will be working in the wavelength range of 380 nanometers to 700 nanometers. In future efforts will be made in the direction of making the complete structure of the photonic crystal and to work on different range of frequencies in the visible light region which are being passed through it and make it suitable for the real world applications in the are of visible light communication.

Bibliography

- [1] S. John, “Strong localization of photons in certain disordered dielectric superlattices,” *Phys. Rev. Lett.*, vol. 58, no. 23, pp. 2486–2489, 1987.
- [2] E. Yablonovitch, “Inhibited spontaneous emission in solid-state physics and electronics,” *Phys. Rev. Lett.*, vol. 58, no. 20, pp. 2059–2062, 1987.
- [3] S. P. Kuo and J. Faith, “Interaction of an electromagnetic wave with a rapidly created spatially periodic plasma,” *Phys. Rev. E, Stat. Phys. Plasmas Fluids Relat. Interdiscip. Top.*, vol. 56, no. 2, pp. 2143–2150, 1997.
- [4] M. Koshiba, “Full-vector analysis of photonic crystal fibers using the finite element method,” *IEICE Trans. Electron.*, vol. E85-C, no. 4, pp. 881–888, 2002.
- [5] H. M. H. Chong and R. M. De La Rue, “Tuning of photonic crystal waveguide microcavity by thermo-optic effect,” *IEEE Photon. Technol. Lett.*, vol. 16, no. 6, pp. 1528–1530, Jun. 2004.
- [6] H. Hojo and A. Mase, “Dispersion relation of electromagnetic waves in one-dimensional plasma photonic crystals,” *J. Plasma Fusion Res.*, vol. 80, no. 2, pp. 89–90, 2004.
- [7] M. Qiu, “Photonic band structures for surface waves on structured metal surfaces,” *Opt. Exp.*, vol. 13, no. 19, pp. 7583–7588, 2005.
- [8] O. Sakai, T. Sakaguchi, Y. Ito, and K. Tachibana, “Interaction and control of millimetre-waves with microplasma arrays,” *Plasma Phys. Controlled Fusion*, vol. 47, no. 12B, pp. B617–B627, 2005.
- [9] L. Shiveshwari and P. Mahto, “Photonic band gap effect in one-dimensional plasma dielectric photonic crystals,” *Solid State Commun.*, vol. 138, no. 3, pp. 160–164, 2006.

- [10] S. Prasad, V. Singh, and A. K. Singh, "Effect of inhomogeneous plasma density on the reflectivity in one dimensional plasma photonic crystal," *Progr. Electromagn. Res. M*, vol. 21, pp. 211–222, Oct. 2011.
- [11] J. Kitagawa, M. Kodama, S. Koya, Y. Nishifuji, D. Armand, and Y. Kadoya, "THz wave propagation in two-dimensional metallic photonic crystal with mechanically tunable photonic-bands," *Opt. Exp.*, vol. 20, no. 16, pp. 17271–17280, 2012.
- [12] B. Guo, M. Q. Xie, and L. Peng, "Photonic band structures of onedimensional photonic crystals doped with plasma," *Phys. Plasmas*, vol. 19, no. 7, p. 072111, 2012.
- [13] L. Qi, L. Shang, and S. Zhang, "One-dimensional plasma photonic crystals with sinusoidal densities," *Phys. Plasmas*, vol. 21, no. 1, p. 013501, 2014.
- [14] J. Luo et al., "Ultratransparent media and transformation optics with shifted spatial dispersions," *Phys. Rev. Lett.*, vol. 117, no. 22, p. 223901, 2016.
- [15] J. C. Knight, "Photonic crystal fibres," *Nature*, vol. 424, no. 6950, pp. 847–851, 2003.
- [16] H. Hojo and A. Mase, "Electromagnetic-wave transmittance characteristics in one-dimensional plasma photonic crystals," *J. Plasma Fusion Res.*, vol. 8, pp. 477–479, Jan. 2009.
- [17] L. Zhang and J.-T. Ouyang, "Experiment and simulation on one-dimensional plasma photonic crystals," *Phys. Plasmas*, vol. 21, no. 10, p. 103514, 2014.
- [18] Haiyun Tan, Chenggang Jin, Lanjian Zhuge, Xuemei Wu, "Simulation on the Photonic Bandgap of 1-D Plasma Photonic Crystals," *IEEE Transaction on plasma science*, vol. 46, no. 3, March 2018.

ORIGINALITY REPORT

18%

SIMILARITY INDEX

9%

INTERNET SOURCES

12%

PUBLICATIONS

7%

STUDENT PAPERS

PRIMARY SOURCES

- 1** Haiyun Tan, Chenggang Jin, Lanjian Zhuge, Xuemei Wu. "Simulation on the Photonic Bandgap of 1-D Plasma Photonic Crystals", IEEE Transactions on Plasma Science, 2018
Publication 4%
- 2** www.ppgeti.ufc.br
Internet Source 3%
- 3** Submitted to American University in Cairo
Student Paper 2%
- 4** Submitted to Indian Institute of Technology, Ropar
Student Paper 1%
- 5** Submitted to Indian School of Mines
Student Paper 1%
- 6** Submitted to Emirates College of Technology
Student Paper 1%
- 7** Lin Zhang, Ji-Ting Ouyang. "Experiment and simulation on one-dimensional plasma photonic crystals", Physics of Plasmas, 2014 1%

8

O Sakai, T Sakaguchi, Y Ito, K Tachibana.
"Interaction and control of millimetre-waves
with microplasma arrays", Plasma Physics and
Controlled Fusion, 2005

Publication

9

V.F. Rodriguez-Esquerre, M. Koshiba, H.E.
Hernandez-Figueroa. "Finite-element analysis
of photonic Crystal cavities: time and frequency
domains", Journal of Lightwave Technology,
2005

Publication

10

www.jpier.org
Internet Source

<1%

11

www.science.gov
Internet Source

<1%

12

Submitted to Malaviya National Institute of
Technology
Student Paper

<1%

13

ethesis.nitrkl.ac.in
Internet Source

<1%

14

Min Qiu. "Photonic band structures for surface
waves on structured metal surfaces", Optics
Express, 2005

Publication

<1%

15

Internet Source

<1%

16

Photonic Crystals and Light Localization in the 21st Century, 2001.

Publication

<1%

17

mems.utdallas.edu

Internet Source

<1%

18

publikationen.bibliothek.kit.edu

Internet Source

<1%

19

Hu, . "Fundamental Properties of Photonic Crystals", Photonic Crystals, 2014.

Publication

<1%

20

tel.archives-ouvertes.fr

Internet Source

<1%

21

osaptesting.osa.org

Internet Source

<1%

22

Eli Yablonovitch. "Inhibited Spontaneous Emission in Solid-State Physics and Electronics", Physical Review Letters, 05/1987

Publication

<1%

23

Submitted to Associatie K.U.Leuven

Student Paper

<1%

24

B. Guo, M. Q. Xie, L. Peng. "Photonic band structures of one-dimensional photonic crystals doped with plasma", Physics of Plasmas, 2012

<1%

25

www.j3.jstage.jst.go.jp

Internet Source

<1%

26

X.Y. Wang, I.J. Lou, C. Lu, P. Shum, C.L. Zhao, P.R. Chaudhuri, M. Yan. "Full-vector analysis of photonic crystal fibers using the boundary element method", Fourth International Conference on Information, Communications and Signal Processing, 2003 and the Fourth Pacific Rim Conference on Multimedia. Proceedings of the 2003 Joint, 2003

Publication

<1%

27

Submitted to Staffordshire University

Student Paper

<1%

28

elpub.bib.uni-wuppertal.de

Internet Source

<1%

29

Bernardo Y. Dantas-Yoshida, V. F. Rodriguez-Esquerre, J. J. Isidio-Lima. "Thermal effects in photonic crystals resonant cavities", 2013 SBMO/IEEE MTT-S International Microwave & Optoelectronics Conference (IMOC), 2013

Publication

<1%

30

Elahe Ataei, Mehdi Sharifian, Najmeh Zare Bidoki. "Magnetized plasma photonic crystals band gap", Journal of Plasma Physics, 2014

Publication

<1%

31

Submitted to University of Nottingham

Student Paper

<1%

32

Hai-Feng Zhang, Shao-Bin Liu. "Magneto-Optical Faraday Effects in Dispersive Properties and Unusual Surface Plasmon Modes in the Three-Dimensional Magnetized Plasma Photonic Crystals", IEEE Photonics Journal, 2014

Publication

<1%

33

S. P. Kuo. "Interaction of an electromagnetic wave with a rapidly created spatially periodic plasma", Physical Review E, 08/1997

Publication

<1%

34

Li, Chun-zao, Shao-bin Liu, Xiang-kun Kong, Hai-feng Zhang, Bo-rui Bian, and Xue-yong Zhang. "A Novel Comb-Like Plasma Photonic Crystal Filter in the Presence of Evanescent Wave", IEEE Transactions on Plasma Science, 2011.

Publication

<1%

35

Submitted to University of Sheffield

Student Paper

<1%

36

citeseerx.ist.psu.edu

Internet Source

<1%